JVI Accepted Manuscript Posted Online 3 August 2016
J. Virol. doi:10.1128/JVI.01133-16
Copyright © 2016, American Society for Microbiology. All Rights Reserved.

Accepted Manuscript Posted Online

Journal of Virology

JVI

Journal of Virology

Downloaded from http://jvi.asm.org/ on August 6, 2016 by NORTHERN ILLINOIS UNIV

Title: Carcinoembryonic Antigen-related Cell Adhesion Molecule 5 (CEACAM5) Is an Important Surface Attachment Factor Facilitating the Entry of the Middle East Respiratory Syndrome Coronavirus (MERS-CoV)

Che-Man Chan[1,2*], Hin Chu[1,2*], Yixin Wang[2], Bosco Ho-Yin Wong[2], Xiaoyu Zhao[2], Jie Zhou[1,2], Dong Yang[2], Sze Pui Leung[2], Jasper Fuk-Woo Chan[1,2,3,4], Man-Lung Yeung[1,2], Jinghua Yan[5], Guangwen Lu[5], George Fu Gao[5], Kwok-Yung Yuen[1,2,3,4,6#].

Affiliations: [1] State Key Laboratory of Emerging Infectious Diseases; [2] Department of Microbiology; [3] Research Centre of Infection and Immunology; [4] Carol Yu Centre for Infection; The University of Hong Kong, Hong Kong Special Administrative Region, China; [5] CAS Key Laboratory of Pathogenic Microbiology and Immunology, Institute of Microbiology, Chinese Academy of Sciences, Beijing 100101, China; [6] The Collaborative Innovation Center for Diagnosis and Treatment of Infectious Diseases, Zhejiang University, Hangzhou, China.

[*] C.-M.C. and H.C. contributed equally to this study.

Running title: CEACAM5 Facilitates MERS-CoV Entry

Word count: Text: 5845. Abstract: 231.

[#]**Correspondence:** Kwok-Yung Yuen, State Key Laboratory of Emerging Infectious Diseases, Carol Yu Centre for Infection, Department of Microbiology, The University of Hong Kong, Queen Mary Hospital, 102 Pokfulam Road, Pokfulam, Hong Kong Special Administrative Region, China. Tel: 852-22554897. Fax: 852-28551241. Email: kyyuen@hku.hk

Accepted Manuscript Posted Online

Journal of Virology

JVI

Journal of Virology

Downloaded from http://jvi.asm.org/ on August 6, 2016 by NORTHERN ILLINOIS UNIV

Abstract

The spike proteins of coronaviruses are capable of binding to a wide range of cellular targets, which contribute to the broad species tropism of coronaviruses. Previous reports have demonstrated that Middle East respiratory syndrome coronavirus (MERS-CoV) predominantly utilizes dipeptidyl peptidase-4 (DPP4) for cell entry. However, additional cellular binding targets of the MERS-CoV spike protein that may augment MERS-CoV infection have not been further explored. In the current study, using the virus overlay protein binding assay (VOPBA), we identified carcinoembryonic antigen-related cell adhesion molecule 5 (CEACAM5) as a novel cell surface binding target of MERS-CoV. CEACAM5 co-immunoprecipitated with the spike protein of MERS-CoV in both overexpressed and endogenous settings. Disrupting the interaction between CEACAM5 and MERS-CoV spike with anti-CEACAM5 antibody, recombinant CEACAM5 protein, or siRNA knockdown of CEACAM5 significantly inhibited the entry of MERS-CoV. Recombinant expression of CEACAM5 did not render the non-permissive baby hamster kidney (BHK21) cells susceptible to MERS-CoV infection. Instead, CEACAM5 overexpression significantly enhanced the attachment of MERS-CoV to the BHK21 cells. More importantly, the entry of MERS-CoV was increased when CEACAM5 was overexpressed in permissive cells, which suggested that CEACAM5 could facilitate MERS-CoV entry in conjunction with DPP4 despite not being able to support MERS-CoV entry independently. Taken together, our study identified CEACAM5 as a novel cell surface binding target of MERS-CoV that facilitates MERS-CoV infection through augmenting the attachment of the virus to the host cell surface.

Accepted Manuscript Posted Online

Journal of Virology

JVI

Journal of Virology

Downloaded from http://jvi.asm.org/ on August 6, 2016 by NORTHERN ILLINOIS UNIV

47 **Importance**

48 Infection with the Middle East respiratory syndrome coronavirus (MERS-CoV) is
49 associated with the highest mortality rate among all known human-pathogenic
50 coronaviruses. Currently, there are no approved vaccines or therapeutics against MERS-
51 CoV infection. The identification of carcinoembryonic antigen-related cell adhesion
52 molecule 5 (CEACAM5) as a novel cell surface binding target of MERS-CoV advanced
53 our knowledge on the cell binding biology of MERS-CoV. Importantly, CEACAM5
54 could potentiate the entry of MERS-CoV through functioning as an attachment factor. In
55 this regard, CEACAM5 could serve as a novel target in addition to dipeptidyl peptidase-4
56 (DPP4) in the development of antiviral strategies for MERS-CoV.
57
58
59
60
61
62
63
64
65
66
67
68
69

Accepted Manuscript Posted Online

Journal of Virology

JVI

Journal of Virology

Downloaded from http://jvi.asm.org/ on August 6, 2016 by NORTHERN ILLINOIS UNIV

70 **Introduction**

71 Coronaviruses are enveloped, positive-sense, and single stranded RNA viruses with
72 genome size of approximately 30kb. They belong to the *Coronaviridae* family under the
73 order of *Nidovirales* and are currently classified into four major genera, including the α,
74 β, γ, and δ genus (1). Coronaviruses can infect a wide range of mammals as well as birds
75 (2). The broad species tropism is predominantly attributed to the high diversity in
76 receptor usage across different coronaviruses. To date, six coronaviruses are known to
77 infect humans and they utilize different surface molecules for cell entry. In particular,
78 human coronavirus 229E (HCoV-229E) binds aminopeptidase N (APN) (3) and human
79 coronavirus OC43 (HCoV-OC43) binds O-acetylated sialic acid (4). Severe acute
80 respiratory syndrome coronavirus (SARS-CoV) (5) and human coronavirus NL63
81 (HCoV-NL63) (6) both binds angiotensin I converting enzyme 2 (ACE2). The receptor
82 for human coronavirus HKU1 (HCoV-HKU1) has not been defined. However, O-
83 acetylated sialic acid has been suggested as an attachment factor that contributes to the
84 binding of HCoV-HKU1 to the cell surface (7). The Middle East respiratory syndrome
85 coronavirus (MERS-CoV) is the sixth coronavirus known to cause infection in humans
86 (8). Intriguingly, MERS-CoV utilizes a unique cellular receptor, dipeptidyl peptidase-4
87 (DPP4), for virus entry (9). The host cell receptors for a number of animal coronaviruses
88 have also been identified. For instance, porcine transmissible gastroenteritis coronavirus
89 (TGEV) binds APN (10) and the prototype β-coronavirus mouse hepatitis virus (MHV)
90 uses carcinoembryonic antigen-related cell adhesion molecule 1 (CEACAM1) for entry
91 (11).
92

Accepted Manuscript Posted Online

Journal of Virology

JVI

Journal of Virology

Downloaded from http://jvi.asm.org/ on August 6, 2016 by NORTHERN ILLINOIS UNIV

93 Coronaviruses have evolved complex receptor recognition patterns. In addition to the
94 defined receptors essential for virus entry into host cells, multiple co-receptors or
95 attachments factors have been reported to play critical roles in the propagation of
96 coronaviruses. In this regard, sialic acids (12) and glycoproteins (13) facilitate the
97 binding of TGEV to target cells in addition to APN. Similarly, HCoV-NL63 utilizes
98 heparan sulfate proteoglycans for attachment to target cells (14). Apart from ACE2,
99 SARS-CoV can also enter cells through liver/lymph node-specific intercellular adhesion
100 molecule-3-grabbing integrin (L-SIGN) (15) and dendritic cell-specific intercellular
101 adhesion molecule-3-grabbing non-integrin (DC-SIGN) (16). Additionally, we have
102 previously identified major histocompatibility complex class I C (HLA-C) as an
103 attachment factor for HCoV-HKU1 that facilitates the entry of the virus (17).
104
105 The emerging MERS-CoV is associated with the highest mortality rate of more than 30%
106 among all known human-pathogenic coronaviruses in inflicted patients and there is as yet
107 no approved treatment regimens or vaccine for MERS (18, 19). As of May 16th 2016,
108 MERS-CoV has caused 1733 laboratory-confirmed cases of human infection, including at
109 least 628 deaths (20). Clinical features of severe MERS include high fever, pneumonia,
110 acute respiratory distress syndrome (ARDS), as well as extrapulmonary manifestations
111 including gastrointestinal symptoms, lymphopenia, acute kidney injury, hepatic
112 inflammation, and pericarditis (21). In agreement with these clinical observations, recent
113 *in vitro* and *in vivo* studies have highlighted the extraordinarily wide range of tissue and
114 cell tropism of MERS-CoV, which is unparalleled by other coronaviruses (22-24).
115 Following the identification of DPP4 as the receptor of MERS-CoV, the broad tissue

Accepted Manuscript Posted Online

Journal of Virology

JVI

Journal of Virology

Downloaded from http://jvi.asm.org/ on August 6, 2016 by NORTHERN ILLINOIS UNIV

116 tropism of MERS-CoV infection is in part explained by the ubiquitous cellular expression
117 of DPP4. However, alternative factors may exist and potentiate the infection of MERS-
118 CoV either in conjunction or independently of DPP4. In this study, we employed the
119 virus overlay protein binding assay (VOPBA) followed by liquid chromatography-
120 tandem mass spectrometry (LC-MS/MS) approach to identify novel cell surface binding
121 targets of MERS-CoV. Our data demonstrated carcinoembryonic antigen-related cell
122 adhesion molecule 5 (CEACAM5) as a novel attachment factor that facilitated MERS-
123 CoV entry. Importantly, interrupting the interaction between CEACAM5 and MERS-
124 CoV-spike inhibited virus entry. Overexpression of CEACAM5 did not grant entry but
125 significantly increased the attachment of MERS-CoV on non-permissive cells.
126 Collectively, our study identified CEACAM5 as an important cell surface binding target
127 for MERS-CoV-spike that facilitates host cell entry for MERS-CoV.
128

129 **Materials and Methods**

130 **Cells**. A549, AD293, Huh7, Caco2, and VeroE6 cells were maintained in Dulbecco's
131 Modified Eagle medium (DMEM) supplemented with 10% heat-inactivated fetal bovine
132 serum (FBS), 100 unit/ml penicillin and 100 µg/ml streptomycin. BEAS2B and Calu3
133 cells were maintained in DMEM/F12 supplemented with 10% heat-inactivated FBS, 100
134 unit/ml penicillin and 100 µg/ml streptomycin. BHK21 cells were maintained in
135 Minimum Essential medium (MEM) supplemented with 10% heat-inactivated FBS, 100
136 unit/ml penicillin and 100 µg/ml streptomycin. L929 cells were maintained in MEM
137 supplemented with 20% heat-inactivated FBS, 100 unit/ml penicillin and 100 µg/ml
138 streptomycin. Human primary T cells were isolated from PBMCs with negative selection

Accepted Manuscript Posted Online

Journal of Virology

JVI

Journal of Virology

Downloaded from http://jvi.asm.org/ on August 6, 2016 by NORTHERN ILLINOIS UNIV

139 using the Dynabeads Untouched Human T cells Kit (Invitrogen, USA) as we previously
140 described (25). Isolated T cells were maintained in Roswell Park Memorial Institute
141 medium (RPMI)-1640 supplemented with 10% FBS, 100 ug/ml streptomycin, 100 U/ml
142 penicillin, 1% sodium pyruvate, 1% non-essential amino acids, and were used
143 immediately for infection.
144
145 **Virus.** The EMC/2012 strain of MERS-CoV (passage 8, designated MERS-CoV) was
146 provided by Dr. Ron Fouchier (Erasmus Medical Center) and cultured with VeroE6 cells
147 with serum free DMEM supplemented with 100 unit/ml penicillin and 100 µg/ml
148 streptomycin. Three days post virus inoculation, culture supernatants were collected,
149 aliquoted, and stored at -80ºC. To determine virus titer, aliquots of MERS-CoV were
150 used for plaque assays on confluent VeroE6 cells in 24-well plates. In brief, MERS-CoV
151 stocks were 10-fold serially diluted in DMEM. Diluted MERS-CoV was then added to
152 duplicate wells of 24-well plates at a volume of 200µl. After inoculating for 1 hour at
153 37ºC, the inoculum was removed from the wells and an agarose overlay was added to the
154 cells. The cells would then be incubated for approximately 72 hours. To count plaques,
155 the cells were fixed with 4% paraformaldehyde for 5 hours and stained with crystal
156 violet.
157
158 **Antibodies.** Rabbit anti-human DPP4, rabbit anti-human CEACAM5, rabbit control IgG
159 (Abcam, USA), and mouse anti-human β-actin (Immunoway, USA) were used in the
160 relevant experiments. MERS-CoV NP was detected with the guinea pig anti-MERS-CoV
161 NP serum as we previously described (25). MERS-CoV spike was detected either with

Accepted Manuscript Posted Online

Journal of Virology

JVI

Journal of Virology

Downloaded from http://jvi.asm.org/ on August 6, 2016 by NORTHERN ILLINOIS UNIV

162 the in-house mouse anti-MERS-CoV spike immune serum or with a rabbit anti-MERS-
163 CoV spike antibody (Sino Biological, China). Secondary antibodies including Alexa
164 Fluor 488/647 goat anti-guinea pig and Alexa Fluor 488/647 goat anti-rabbit (Life
165 Technologies, USA) were used for flow cytometry. Goat anti-mouse HRP (Abcam, USA)
166 was used for Western blot.
167
168 **Plasmid construction.** The synthetic human codon-optimized S gene was used as a
169 template for the construction of all MERS-CoV-S plasmids. For pcDNA-MERS-CoV-S
170 used in producing MERS-S-pseudotyped virus, the full-length S from the N-terminal
171 KpnI site to the C-terminal XhoI site was subcloned to generate full-length S in pcDNA
172 3.1(+). For the construction of the S1 plasmid (amino acids 1-925), the 5' forward primer
173 sequence containing a BSSHII site (5'GCGCGCCACCATGATACACTC
174 AGTGTTTCTACTGATGTTC) was used together with the 3' reverse primer (5'-
175 GGGCCCATCACCGTCTTCCCACACAGTGGATG) with a ApaI site. The fragment
176 was PCR amplified and cloned into the pSFV1 vector (kindly provided by Dr. P.
177 Liljestrom) with the C terminus fused in-frame with the FLAG sequence (DYKDDDDK)
178 and resulting in the plasmid pSFV-MERS-CoV-S1-FLAG. For the construction of the
179 pSFV-DPP4-6xHis plasmid, forward primer containing a BSSHII site (5'-
180 GCGCGCCACCATGAAGACACCGTGGAAGG) and reverse primer with a ApaI site
181 (5'- GGGCCCAGGTAAAGAGAAACATTGTTTTATG) were used. The fragment was
182 cloned into the pSFV1 vector with the 6x His sequence (HHHHHH) fused in-frame at the
183 C-terminus. For the construction of the pcDNA-DPP4, the forward primer containing a
184 KpnI site (5'-TAAGCAGGTACCGCCACCATGAAGACACCGTGGAAGGTTCT) and

Accepted Manuscript Posted Online

Journal of Virology

JVI

Journal of Virology

Downloaded from http://jvi.asm.org/ on August 6, 2016 by NORTHERN ILLINOIS UNIV

185 the reverse primer containing a EcoRI site (5'-
186 TGCTTAGAATTCCTAAGGTAAAGAGAAACATTGTTTTATGAAGTGGC) were
187 used to insert the full-length human DPP4 into the pcDNA3.1(+) vector between the
188 KpnI and the EcoRI sites. For the construction of pcDNA-CEACAM5-V5, the forward
189 primer (5'GATATCCACCATGGAGTCTCCCTCGGCCCCTCCCCAC') contains the
190 N-terminal signal sequence, the EcoRV site, and the Kozak sequence. The reverse-primer
191 (5'- CTCGAGTATCAGAGCAACCCCAACCAGCACTCC) contains the XhoI site at
192 the C-terminal cytoplasmic domain. The amplified fragment was used to generate full
193 length CEACAM5 in pcDNA 3.1(+) with a V5 tag (GKPIPNPLLGLDST) in-frame at the
194 C-terminus, resulting in pcDNA-CEACAM5-V5.
195
196 **Production of MERS-S-pseudotyped virus.** Lentivirus-based MERS-S-pseudotyped
197 virus was generated by co-transfecting 293FT cells with pcDNA-MERS-full length spike
198 in combination with pNL4-3-R$^-$.E$^-$, which is a HIV backbone plasmid bearing the
199 luciferase reporter gene. pNL4-3-R$^-$.E$^-$ was obtained through the NIH AIDS research and
200 reference reagents program. The viral particles in supernatant were harvested at 48 hours
201 post transfection by ultra-centrifugation in 30% sucrose solution in Beckman rotor
202 SW32Ti at the speed of 32,000 rpm for 1 hour at 4ºC (17). The p24 concentrations were
203 quantified with a p24 antigen enzyme-linked immunoassay kit (Cell Biolabs, USA) and
204 stored in aliquots at -80ºC. Pseudovirus titer was quantified in unit of lentiviral particle
205 (LP) per ml according to the manufacturer's instruction.
206

Accepted Manuscript Posted Online

Journal of Virology

JVI

Journal of Virology

Downloaded from http://jvi.asm.org/ on August 6, 2016 by NORTHERN ILLINOIS UNIV

207 **Virus Overlay Protein Binding Assay (VOPBA) and Western Blot.** Confluent A549
208 cells in 75 cm^2 tissue flask were washed three times in chilled PBS, surface-biotinylated,
209 and extracted using Pierce Cell Surface Protein Isolation Kit (Thermo Scientific, USA)
210 according to the manufacturer's protocol. Biotinylated membrane extracts were bound
211 onto neutrAvidin agarose resin (Thermo Scientific, USA), washed, and eluted in LDS
212 sample buffer (Invitrogen, USA). After electrophoresis into 4-12% gradient NuPAGE
213 SDS-PAGE Gel (Invitrogen, USA) under reducing condition, biotinylated surface
214 extracts were electro-transferred onto Hybond-PVDF membranes (GE Healthcare, UK)
215 for 2 hours at constant voltage of 30 V at 4ºC. Membrane was blocked in 10% skim milk
216 (Oxoid, UK) in PBS at 4ºC overnight on a rotator. The membrane was then incubated
217 with 1% skim milk solution containing MERS-S-pseudotyped virus at 10^9 lentiviral
218 particles/ml for 2 hours. Membrane was washed twice in 10% skim milk, once in PBS
219 and incubated with rabbit antiserum raised against MERS-CoV spike protein at 1 µg/ml
220 for 2 hours at room temperature. After incubating with the spike-specific antibody, we
221 washed the membrane twice in 10% skim milk, once in PBS, and incubated with PBS
222 containing 1:5000 goat anti-rabbit-800 infra-red dye (LI-COR, USA). Membranes were
223 scanned with an Odyssey Imaging System (LI-COR, USA). The visualized reactive
224 protein detected by VOPBA on Western blot was excised from the gel. The gel piece was
225 inserted into dialysis tubing and filled with 1X MOPS SDS running buffer. Protein
226 contents were electro-eluted at a constant voltage of 50V for 6 hours, collected, dialyzed
227 overnight at 4ºC against PBS in Slide-A-Lyzer Cassette (Thermo Scientific, USA) and
228 concentrated using Microcon columns (Millipore, USA). Eluted contents were
229 electrophoresed and confirmed by VOPBA. The gel fragment was excised for LC-

Accepted Manuscript Posted Online

Journal of Virology

JVI

Journal of Virology

Downloaded from http://jvi.asm.org/ on August 6, 2016 by NORTHERN ILLINOIS UNIV

230 MS/MS analysis carried out in the Center for Genomic Sciences at the University of
231 Hong Kong as we previously described (26).
232
233 **Co-immunoprecipitation (co-IP).** Co-IP was performed using anti-FLAG M2 affinity
234 gel beads (Sigma, USA) or V5 antibody pre-adsorbed to Protein A+G sepharose (Thermo
235 Scientific, USA). Cell lysates were harvested in lysis buffer (20 mM Tris-HCl [pH 7.4],
236 150mM NaCl, 1% Triton X-100, 0.1% NP-40, protease and phosphatase inhibitors
237 cocktails, Roche). Lysed cells were incubated on ice for 15-30 min and then centrifuged.
238 Supernatant was added to antibody-coupled beads or anti-FLAG affinity gel beads and
239 incubated overnight at 4ºC. Beads were washed three times with lysis buffer and Western
240 blot was performed. Immunoprecipitated products or cell lysates were mixed with SDS
241 loading buffer and heated at 95ºC for 10 min. Samples were fractionated in 10% SDS-
242 PAGE and then transferred onto PVDF membranes (GE Healthcare, UK). After blocking
243 overnight with 10% skim milk, membranes were incubated with corresponding primary
244 antibodies and then with infra-red dye conjugated secondary antibodies (LI-COR, USA).
245 Membranes were scanned with an Odyssey Imaging System (LI-COR, USA).
246
247 **Quantitative RT-PCR.** Cells were lysed in RLT buffer with 40mM DTT and extracted
248 with the RNeasy mini kit (Qiagen, USA). Viral RNA in the supernatant was extracted
249 with the PureLink Viral RNA/DNA mini kit (Life Technologies, USA). Reverse
250 transcription (RT) and quantitative polymerase chain reaction (qPCR) were performed
251 with the Transcriptor First Strand cDNA Synthesis kit and LightCycler 480 master mix
252 from Roche as we previously described (27, 28). In the RT reactions, reverse primers

Accepted Manuscript Posted Online

Journal of Virology

JVI

Journal of Virology

Downloaded from http://jvi.asm.org/ on August 6, 2016 by NORTHERN ILLINOIS UNIV

253 against the NP gene of MERS-CoV were used to detect cDNA complementary to the
254 positive strand of viral genomes. The following sets of primers were used to detect NP in
255 qPCR.
256 (F) 5'- CAAAACCTTCCCTAAGAAGGAAAAG-3'
257 (R) 5'- GCTCCTTTGGAGGTTCAGACAT-3'
258 (Probe) FAM 5'-ACAAAAGGCACCAAAAGAAGAATCAACAGACC-3' BHQ1
259
260 **Antibody blocking assays.** The antibody blocking assay based on the MERS-S-
261 pseudotyped virus was performed by measuring the infection of target cells with the use
262 of luciferase as a reporter gene (17). In brief, antibody was diluted to 2µg/ml in serum
263 free culture medium and incubated with Calu3 cells for 1 hour at 37ºC. Pseudotyped virus
264 was added to target cells at a ratio of 100 lentiviral particle (LP) per cell and the inoculum
265 was replaced with fresh medium with 10% FBS after 1 hour. Luciferase activity was
266 determined at 48 hours post infection. For the antibody blocking assay based on the
267 infectious MERS-CoV, Calu3 cells were pre-incubated with rabbit polyclonal anti-
268 CEACAM5 at different concentrations ranging from 0.5-4 µg/ml. Rabbit polyclonal anti-
269 DPP4 at 4 µg/ml and rabbit IgG at 4µg/ml were included as controls. After pre-incubating
270 with the antibodies for 1 hour at 37ºC, the cells were challenged with MERS-CoV at 1
271 MOI for 1 hour at 37ºC in the presence of antibodies. The cells were subsequently
272 washed with PBS and lysed with RLT with 40mM dithiothreitol (DTT). To determine the
273 impact of antibody blocking on MERS-CoV multi-cycle replication, Huh7 cells were pre-
274 incubated with 2 µg/ml anti-CEACAM5 antibody, anti-DPP4 antibody, or rabbit IgG.
275 After the pre-incubation, the cells were infected with MERS-CoV at 0.0005 MOI for 1

Accepted Manuscript Posted Online

Journal of Virology

JVI

Journal of Virology

Downloaded from http://jvi.asm.org/ on August 6, 2016 by NORTHERN ILLINOIS UNIV

276 hour at 37ºC in the presence of antibodies. The cells were then washed in PBS and
277 replenished with DMEM with blocking antibodies. Infected cells were incubated at 37ºC
278 and harvested at 1, 24, and 48 hours post infection. The virus copy number was
279 determined with qPCR.
280
281 **Human recombinant protein blocking assays.** Human recombinant proteins (DPP4,
282 CEACAM5, and control IgG) were obtained from Sino Biological. MERS-CoV was pre-
283 incubated with human recombinant proteins (5 µg/ml to 40 µg/ml for CEACAM5, 40
284 µg/ml for DPP4, and 40 µg/ml for control IgG) for 1 hour before inoculating onto Calu3
285 and Huh7 cells. The protein-virus complexes were then incubated with Calu3 and Huh7
286 cells for 2 hours at 37ºC. After the incubation period, the inoculum was discarded and the
287 cells were washed with PBS followed by lysing in RLT with 40mM DTT. The virus copy
288 number was determined with qPCR.
289
290 **siRNA knockdown.** Silencer Select siRNA human CEACAM5 siRNA, Silencer Select
291 siRNA human DPP4 siRNA, and Silencer Select siRNA negative control were obtained
292 from Life Technologies. Transfection of siRNA on Huh7 cells was performed using
293 Lipofectamine 3000 (Thermo Fisher, USA) following manufacturer's manual. In brief,
294 Huh7 cells were transfected with 100µM siRNA for two consecutive days. At 24 hours
295 post the second siRNA transfection, the cells were challenged with MERS-CoV at 1 MOI
296 for 2 hours at 37ºC. Following the incubation, the cells were washed with PBS and lysed
297 in RLT with 40mM DTT. The virus copy number was determined with qPCR.
298

Accepted Manuscript Posted Online

Journal of Virology

JVI

Journal of Virology

Downloaded from http://jvi.asm.org/ on August 6, 2016 by NORTHERN ILLINOIS UNIV

299 **Flow cytometry.** All samples were detached with 10mM EDTA and fixed in 4%
300 paraformaldehyde. Cell permeabilization for intracellular staining was performed with
301 0.1% Triton X-100 in PBS. Immunostaining for flow cytometry was performed following
302 standard procedures as we previously described (29). The flow cytometry was performed
303 using a BD FACSCanto II flow cytometer (BD Biosciences, USA) and data was analyzed
304 using FlowJo vX (Tree Star, USA).
305
306 **Flow cytometry of BHK21 cells with overexpression of DPP4 and CEACAM5.**
307 BHK21 cells were transfected with pSFV-DPP4 or pcDNA-CEACAM5. The transfected
308 cells were inoculated with MERS-CoV at 48 hours post transfection. To determine virus
309 entry, the cells were inoculated with MERS-CoV at 5 MOI at 37ºC for 2 hours. After 2
310 hours, the cells were washed with PBS and incubated for another 4 hours. At 6 hours
311 post-infection, the cells were washed extensively with PBS, fixed in 4%
312 paraformaldehyde, and immunolabeled for flow cytometry. To determine virus
313 attachment, the cells were inoculated with MERS-CoV at 30 MOI at 4ºC for 2 hours.
314 After 2 hours, the cells were washed with PBS, fixed in 4% paraformaldehyde, and
315 immunolabeled for flow cytometry.
316
317 **Confocal microscopy.** This study was approved by the Institutional Review Board of the
318 University of Hong Kong/Hospital Authority Hong Kong West Cluster. Normal human
319 lung sections were deparaffinized and rehydrated following standard procedures. Antigen
320 unmasking was performed by boiling tissue sections with the antigen unmasking solution
321 from Vector Laboratories. Goat anti-DPP4 was obtained from R&D and rabbit anti-

Accepted Manuscript Posted Online

Journal of Virology

JVI

Journal of Virology

Downloaded from http://jvi.asm.org/ on August 6, 2016 by NORTHERN ILLINOIS UNIV

322 CEACAM5 was obtained from Abcam. Secondary antibodies were obtained from Life
323 Technologies. Mounting and DAPI staining were performed with the Vectashield
324 mounting medium (Vector Laboratories). Images were acquired with a Carl Zeiss LSM
325 780 system.
326
327 **Statistical analysis.** Data on figures represented means and standard deviations.
328 Statistical comparison between different groups was performed by Student's *t*-test using
329 GraphPad Prism 6. Differences were considered statistically significant when $p < 0.05$.
330
331 **Results**
332 **Identification of CEACAM5 as a cell surface binding protein of MERS-CoV**
333 To probe for potential cell surface factors that can interact with MERS-CoV, we
334 employed the virus overlay protein binding assay (VOPBA), which we have previously
335 utilized to identify host cell surface binding proteins of the influenza A virus (26). In
336 brief, membrane proteins on A549 cells were selectively biotinylated and separated from
337 non-biotinylated intracellular proteins by binding to avidin agarose (23). The biotinylated
338 A549 surface extracts separated in 4-12% gradient SDS NuPAGE gel were transferred to
339 PVDF membrane before incubating with MERS-S-pseudotyped viruses for 2 hours at
340 room temperature (Figure 1A). Subsequently, reactive signals were revealed with a rabbit
341 polyclonal antibody against MERS-CoV spike. As shown in figure 1B, VOPBA revealed
342 several reactive bands from A549 surface extracts including two prominent bands at
343 molecular sizes of approximately 120 and 90 kDa (lane 1) but not from the control
344 NIH3T3 cell (lane 2), which is not permissive for MERS-CoV infection (30). In order to

Accepted Manuscript Posted Online

Journal of Virology

JVI

Journal of Virology

Downloaded from http://jvi.asm.org/ on August 6, 2016 by NORTHERN ILLINOIS UNIV

345 confirm the immunoreactivity of these two proteins to MERS-S-pseudotyped virus, the
346 relevant fractions from the SDS-PAGE gel was excised, electro-eluted, and hybridized
347 with MERS-S-pseudotyped virus. Although both proteins reacted with the virus, the
348 protein at around 90 kDa returned a much stronger signal and was selected for subsequent
349 analyses (Figure 1C). Tryptic peptides mass fingerprints derived from the excised band
350 revealed the protein to be human carcinoembryonic antigen-related cell adhesion
351 molecule 5 (CEACAM5) using the MASCOT search engine against NCBI and Swiss-
352 Prot database (Figure 1D).
353
354 **CEACAM5 is expressed on cell types that are highly susceptible to MERS-CoV**
355 Most CEACAMs are considered as modulators of general cellular processes including
356 proliferation, motility, apoptosis, attachment, as well as cell-cell interaction. In addition,
357 CEACAM5 may also play roles in innate immune defense by binding and trapping
358 microorganisms (31). To verify the relevance of CEACAM5 in MERS-CoV entry, we
359 investigated the expression of CEACAM5 on a number of cell types. To this end,
360 different cell types in 6-well plates were detached with EDTA, washed, and fixed in 4%
361 paraformaldehyde. Immunostaining for surface CEACAM5 and DPP4 expression were
362 performed without cell permeabilization. The percentage of positive cells and the surface
363 mean fluorescent intensities (MFIs) were determined with flow cytometry. In agreement
364 with previously published reports, DPP4 was detected ubiquitously on different human
365 cell lines (Figure 2A) as well as human primary T cells (Figure 2B). In addition, the
366 polyclonal antibody against human DPP4 also cross-reacted with the DPP4 on a number
367 of non-human mammalian cells, which included VeroE6 (monkey), BHK21 (hamster),

Accepted Manuscript Posted Online

Journal of Virology

JVI

Journal of Virology

Downloaded from http://jvi.asm.org/ on August 6, 2016 by NORTHERN ILLINOIS UNIV

368 and L929 (mouse) cells (Figure 2C). Notably, despite being recognized by the human
369 DPP4 antibody, the DPP4 on hamster and mouse cells do not support MERS-CoV entry
370 (30). In contrast to DPP4, our data demonstrated that the expression of CEACAM5 was
371 more restricted. Among the six human cell lines we analyzed, CEACAM5 expression
372 was detected on A549, Calu3, and Huh7 cells (Figure 2A). At the same time, little to no
373 CEACAM5 expression was detected on AD293, BEAS2B, and Caco2 cells (Figure 2A).
374 Importantly, CEACAM5 expression was also detected on human primary T cells (Figure
375 2B). However, no human CEACAM5 ortholog was expressed on VeroE6, BHK21, and
376 L929 cells (Figure 2C). Quantitatively, CEACAM5 expression was detected
377 predominantly on cells that are highly susceptible to MERS-CoV infection, which
378 include Calu3, Huh7, A549, and T cells (Figure 2D and Figure 2E). Thus, our data
379 supported the notion that CEACAM5 might be an important surface binding protein,
380 which could facilitate MERS-CoV entry.
381
382 **CEACAM5 is co-expressed with DPP4 in human lung tissues**
383 To further verify the physiological relevance of CEACAM5 in MERS-CoV infection, we
384 evaluated the expression of CEACAM5 in human lung tissues and compared the
385 expression with that of DPP4 by immunofluorescent microscopy. Our result revealed that
386 CEACAM5 could be readily detected in the epithelial cells in various regions of the
387 human lung tissues (Figure 3). In particular, colocalization between CEACAM5 and
388 DPP4 was observed in the bronchial epithelium (Figure 3A) but appeared to be more
389 extensive in the epithelium of small airways (Figure 3B). The colocalization between
390 CEACAM5 and DPP4 was also detected in alveoli (Figure 3C) including the alveolar

Accepted Manuscript Posted Online

Journal of Virology

JVI

Journal of Virology

Downloaded from http://jvi.asm.org/ on August 6, 2016 by NORTHERN ILLINOIS UNIV

391 macrophages (Figure 3C, arrowheads). Collectively, the detection of CEACAM5 in the
392 epithelial cells of the human lung tissues and its co-expression with DPP4 in these
393 samples demonstrated the potential capacity of CEACAM5 in facilitating MERS-CoV
394 infection in the lower respiratory tract.
395
396 **CEACAM5 interacts with MERS-CoV spike**
397 To validate our VOPBA-LC-MS/MS findings, the direct interaction between MERS-CoV
398 S1 and CEACAM5 was characterized by co-immunoprecipitation (co-IP). BHK21 cells
399 were either transfected with a CEACAM5-V5 expression vector or a control vector
400 tagged with V5. The surface and intracellular expression of transfected CEACAM-V5
401 was verified with flow cytometry (Figure 4A). Transfected BHK21 cells were then
402 immunoprecipitated with either MERS-CoV S1-FLAG or E. coli bacterial alkaline
403 phosphatase-FLAG (BAP-FLAG) pre-adsorbed onto anti-FLAG M2 agarose beads. The
404 bound protein complexes were spun down, washed, and subjected to Western blot
405 detection with the anti-FLAG (Figure 4B, upper panel) or the anti-V5 antibody (Figure
406 4B, lower panel). As demonstrated in figure 4B, CEACAM5 bound specifically to
407 MERS-CoV S1 (lower panel, lane 1). In contrast, CEACAM5 did not bind to the control
408 bait protein (lower panel, lane 2). At the same time, CEACAM5 was not detected in
409 samples transfected with the empty vector (lower panel, lane 3). In parallel, we
410 performed reciprocal co-IP experiments, in which CEACAM5-V5 was used as the bait
411 instead of MERS-CoV S1-FLAG (Figure 4C). To this end, CEACAM5-V5 or empty
412 vector transfected BHK21 cell lysates were immunoprecipitated with anti-V5 pre-
413 adsorbed protein A/G sepharose, spun down, washed, and incubated with purified

Accepted Manuscript Posted Online

Journal of Virology

JVI

Journal of Virology

Downloaded from http://jvi.asm.org/ on August 6, 2016 by NORTHERN ILLINOIS UNIV

414 MERS-CoV S1-FLAG or BAP-FLAG. Western blot detection with anti-FLAG showed
415 that CEACAM5-V5 interacted with MERS-CoV S1-FLAG (Figure 4C, upper panel, lane
416 1) but not BAP-FLAG (Figure 4C, upper panel, lane 2). As a negative control, the V5
417 empty vector did not pull down MERS-CoV S1 (Figure 4C, upper panel, lane 3). In line
418 with the flow cytometry data from Figure 2C, the antibody against human CEACAM5
419 did not pick up any signal from the BHK21 cell lysates (Figure 4C, lower panel, lane 3).
420 To further validate our findings and avoid the use of overexpressed or tagged fusion
421 proteins, we performed endogenous co-IP on non-transfected Huh7 cells infected with
422 MERS-CoV using antibody against CEACAM5 or MERS-CoV spike. As demonstrated
423 in figure 4D, MERS-CoV spike was detected in infected samples immunoprecipitated
424 with the anti-CEACAM5 antibody. In contrast, MERS-CoV spike was not detected from
425 uninfected samples or from infected samples immunoprecipitated with non-specific rabbit
426 IgG. The interaction between MERS-CoV spike and CEACAM5 was confirmed with
427 reciprocal co-IP using antibody against MERS-CoV spike. In this regard, endogenous
428 CEACAM5 was detected from infected samples immunoprecipitated with antibody
429 against MERS-CoV spike but not from uninfected samples or from infected samples
430 immunoprecipitated with non-specific rabbit IgG (Figure 4D). Take together, our co-IP
431 results demonstrated that MERS-CoV S1 could bind specifically to CEACAM5.
432

433 **CEACAM5-specific antibody blocks MERS-CoV entry and spread**

434 After confirming the direct interaction between CEACAM5 and MERS-CoV S1, we next
435 investigated the potential functional role of CEACAM5 in MERS-CoV entry. We first
436 assessed the capacity of CEACAM5 antibody in blocking the entry of MERS-S-

Accepted Manuscript Posted Online

Journal of Virology

JVI

Journal of Virology

Downloaded from http://jvi.asm.org/ on August 6, 2016 by NORTHERN ILLINOIS UNIV

437 pseudovirus. In this setting, Calu3 cells were pre-incubated with polyclonal antibody
438 against human CEACAM5, or with rabbit IgG and polyclonal antibody against DPP4 as
439 negative and positive controls, respectively. After the pre-incubation, MERS-S-
440 pseudoviruses were inoculated on to the cells for another hour in the presence of the
441 CEACAM5 antibody. Inoculum was replaced with fresh medium with 10% FBS after 1
442 hour and the luciferase activity was determined at 48 hours post infection. As
443 demonstrated in figure 5A, polyclonal antibody against human CEACAM5 at 2 μg/ml
444 significantly reduced the entry of MERS-S-pseudovirus. Next, the antibody blocking
445 experiment was further validated using infectious MERS-CoV under a titration of
446 different CEACAM5 antibody concentrations ranging from 0.5 μg/ml to 4 μg/ml. Our
447 result demonstrated that CEACAM5 antibody blocked the infection of MERS-CoV in a
448 dose-dependent manner (Figure 5B). As a control, antibody added after MERS-CoV
449 inoculation did not affect virus entry (Figure 5C). At the same time, addition of the
450 CEACAM5 antibody did not prevent the entry of MERS-CoV in Caco2 cells, which
451 expressed a low level of CEACAM5 (Figure 5D). To determine the impact of
452 CEACAM5 inhibition on multi-cycle spread of MERS-CoV, we extended the antibody
453 blocking experiment to Huh7 cells. In this scenario, Huh7 cells were pre-incubated with
454 the CEACAM5 antibody for 1 hour and inoculated with MERS-CoV at low MOI in the
455 presence of the CEACAM5 antibody. Infected cells were then washed and incubated in
456 DMEM culture media in the presence of the CEACAM5 antibody. Remarkably, our data
457 suggested that the CEACAM5 antibody significantly reduced MERS-CoV propagation in
458 both cell lysates (Figure 5E) and supernatants (Figure 5F) of infected Huh7 cells. Overall,

Accepted Manuscript Posted Online

Journal of Virology

JVI

Journal of Virology

Downloaded from http://jvi.asm.org/ on August 6, 2016 by NORTHERN ILLINOIS UNIV

459 we demonstrated that CEACAM5 was important for MERS-CoV entry as well as in
460 multi-cycle viral spread.
461
462 **CEACAM5 recombinant protein and siRNA knockdown of CEACAM5 inhibits**
463 **MERS-CoV entry**
464 In addition to antibody blocking, we sought to further verify the impact of CEACAM5
465 inhibition on MERS-CoV infection with alternative approaches including protein
466 blocking and siRNA knockdown. In protein blocking assays, MERS-CoV was pre-
467 incubated with human recombinant CEACAM5 protein ranging from 5 μg/ml to 40
468 μg/ml. Human recombinant DPP4 protein and human recombinant IgG were included as
469 controls. Calu3 or Huh7 cells were subsequently inoculated for 2 hours with the virus-
470 protein mixes. After inoculation, the cells were washed and harvested for viral load
471 quantification with qPCR analysis. Remarkably, our data demonstrated that the human
472 CEACAM5 recombinant protein blocked the entry of MERS-CoV in a dose-dependent
473 manner in both Calu3 (Figure 6A) and Huh7 cells (Figure 6B). As a control, CEACAM5
474 protein added after MERS-CoV inoculation had no effect on virus entry (Figure 6C).
475 Next, we depleted the endogenous expression of CEACAM5 in Huh7 cells with siRNA.
476 The reduction of CEACAM5 surface expression was examined with flow cytometry with
477 no cell permeabilization (Figure 6D). As illustrated in figure 6E and figure 6F, siRNA
478 treatment significantly diminished the surface expression of CEACAM5 both in terms of
479 the percentage of CEACAM5 positive cell (Figure 6E) as well as the mean fluorescent
480 intensity (MFI) (Figure 6F). Notably, when the CEACAM5 siRNA-treated Huh7 cells
481 were challenged with MERS-CoV, we detected a significant decrease in MERS-CoV

Accepted Manuscript Posted Online

Journal of Virology

JVI

Journal of Virology

Downloaded from http://jvi.asm.org/ on August 6, 2016 by NORTHERN ILLINOIS UNIV

482 entry (Figure 6G). Overall, our data from protein blocking and siRNA knockdown
483 experiments corroborated with the findings of the antibody blocking assays, which
484 supported CEACAM5 to be an important cell surface protein in MERS-CoV infection.
485
486 **CEACAM5 is an attachment factor for MERS-CoV**
487 To further define the role of CEACAM5 in MERS-CoV infection, we examined the
488 capacity of CEACAM5 in supporting MERS-CoV entry and attachment. To assess the
489 role of CEACAM5 in MERS-CoV entry, CEACAM5-overexpressing BHK21 cells were
490 inoculated with MERS-CoV at 37ºC for 2 hours. The cells were then washed and
491 incubated at 37ºC for 4 additional hours before harvesting for flow cytometry. Next, to
492 assess the role of CEACAM5 in MERS-CoV attachment, CEACAM5-overexpressing
493 BHK21 cells were inoculated with high MOI MERS-CoV at 4ºC for 2 hours. The
494 infected cells were subsequently washed, harvested, and immunolabeled for flow
495 cytometry. In both cases, DPP4-overexpressing BHK21 cells were included as controls.
496 The result of the entry assessment recapitulated the finding that human DPP4
497 overexpression could support MERS-CoV entry in the otherwise non-permissive BHK21
498 cells. In stark contrast, human CEACAM5-expressing BHK21 cells failed to sustain the
499 entry of MERS-CoV (Figure 7A and Figure 7B). In the attachment assessment, our data
500 suggested that while MERS-CoV could attach to the cell surface of BHK21 cells, human
501 DPP4 overexpression increased the amount of attached virus particles by around 3-folds.
502 Intriguingly, in human CEACAM5-expressing BHK21 cells, the amount of attached virus
503 particles was also significantly increased by more than 2-folds (Figure 7C and Figure
504 7D). To further verify the potential contribution of CEACAM5 in MERS-CoV entry, we

Accepted Manuscript Posted Online

Journal of Virology

JVI

Journal of Virology

Downloaded from http://jvi.asm.org/ on August 6, 2016 by NORTHERN ILLINOIS UNIV

505 overexpressed CEACAM5 in BHK21 and AD293 cells followed by MERS-CoV
506 infection. In corroboration of the result from figure 7A, our data showed that while
507 CEACAM5 enhanced virus attachment to BHK21 cells (Figure 8B), it could not function
508 as an independent receptor for MERS-CoV entry in the non-permissive BHK21 cells
509 (Figure 8A). Perhaps most importantly, overexpression of CEACAM5 increased the entry
510 of MERS-CoV in permissive cells (Figure 8C) in addition to enhancing the attachment of
511 the virus (Figure 8D), which suggested that CEACAM5 could contribute to MERS-CoV
512 entry in conjunction with DPP4. To further investigate if CEACAM5 could facilitate the
513 entry of other human coronaviruses, we challenged CEACAM5-transfected VeroE6 cells
514 (Figure 9A) with SARS-S-pseudovirus and compared pseudovirus entry with that from
515 the empty vector-transfected VeroE6 cells. Our result demonstrated that CEACAM5
516 overexpression did not significantly enhance the entry of SARS-S-pseudovirus (Figure
517 9B). Taken together, our data identified CEACAM5 as an important cell surface binding
518 protein for MERS-CoV that could facilitate the entry of MERS-CoV by acting as an
519 attachment factor.
520

521 **Discussion**

522 The spike proteins of coronaviruses are known to bind a broad range of cellular targets
523 including sialic acids, sugars, and proteins (32). It is now clear that MERS-CoV
524 predominantly utilizes DPP4 for cell entry (9). However, additional cellular binding
525 targets of the MERS-CoV spike protein that may augment MERS-CoV entry have not
526 been further explored. In the current study, using the VOPBA-LC-MS/MS approach, we
527 unveiled CEACAM5 as a novel cell surface binding protein of MERS-CoV (Figure 1).

Accepted Manuscript Posted Online

Journal of Virology

JVI

Journal of Virology

Downloaded from http://jvi.asm.org/ on August 6, 2016 by NORTHERN ILLINOIS UNIV

528 Intriguingly, expression analysis revealed that CEACAM5 were expressed on cell types
529 that are highly permissive to MERS-CoV infection, including Calu3, Huh7, A549, and
530 primary T cells (Figure 2). CEACAM5 and DPP4 co-expressed in the human lung, which
531 highlighted the physiologically relevance of CEACAM5 in MERS-CoV entry (Figure 3).
532 Subsequently, a series of co-IP studies demonstrated the capacity of CEACAM5 in
533 binding to the spike protein of MERS-CoV either in overexpressed or endogenous
534 settings (Figure 4). Remarkably, when the interaction between CEACAM5 and MERS-
535 CoV spike was perturbed with anti-CEACAM5 antibody (Figure 5), recombinant
536 CEACAM5 protein (Figure 6), or CEACAM5 siRNA knockdown (Figure 6), the
537 infection of MERS-CoV was significantly inhibited. Notably, recombinant expression of
538 CEACAM5 did not confer susceptibility of non-permissive BHK21 cells to infection by
539 MERS-CoV (Figure 7A). Instead, CEACAM5 overexpression significantly enhanced the
540 attachment of MERS-CoV to the BHK21 cells (Figure 7B). Perhaps most importantly,
541 the entry of MERS-CoV was increased when CEACAM5 was overexpressed in AD293,
542 which suggested that CEACAM5 could facilitate MERS-CoV entry in conjunction with
543 DPP4 despite being unable to support MERS-CoV entry independently (Figure 8). The
544 interaction between CEACAM5 and MERS-CoV appeared to be specific since
545 CEACAM5 did not facilitate the entry of SARS-CoV (Figure 9). Taken together, our
546 study identified CEACAM5 as a novel cell surface binding protein of MERS-CoV that
547 facilitates MERS-CoV infection through augmenting the attachment of the virus to the
548 cell surface.
549

Accepted Manuscript Posted Online

Journal of Virology

JVI

Journal of Virology

Downloaded from http://jvi.asm.org/ on August 6, 2016 by NORTHERN ILLINOIS UNIV

550 CEACAM family members including CEACAM5 are heavily glycosylated cell surface
551 proteins (33, 34). Currently, 12 members of the CEACAM family have been identified in
552 human. Most CEACAMs are considered as modulators of general cellular processes
553 including proliferation, motility, apoptosis, attachment, as well as cell-cell interaction
554 (35). Notably, aberrant CEACAM function is associated with tumor progression and a
555 number of CEACAMs are utilized as clinical biomarkers. In addition, members of the
556 CEACAM family have been implicated in signal transduction and the binding of bacteria
557 to host target cells. In particular, certain CEACAMs including CEACAM5 are expressed
558 on the apical membrane of epithelial cells and are exploited as receptors or binding
559 factors for a number of pathogenic bacteria (35). Engaging surface CEACAMs by these
560 bacteria not only provides a portal of attachment but also triggers internalization and
561 entry of the bacteria into epithelial cells.
562
563 In the context of coronaviruses, previous reports have identified murine CEACAM1 as
564 the principal cellular receptor of the mouse hepatitis virus (MHV) (11). The discovery of
565 CEACAM5 as a cellular binding target of MERS-CoV spike suggested that perhaps cell
566 surface CEACAMs are common binding targets of coronavirus spikes that can be
567 exploited for attachment or entry. It will be tempting to speculate that other members of
568 the coronavirus family can also make use of certain CEACAMs to facilitate infection.
569 Notably, the spike proteins of coronaviruses are capable of binding to multiple cellular
570 targets. As an example, SARS-CoV binds to ACE2 with the spike S1 C-terminal domain
571 (CTD) (36). At the same time, the SARS-CoV spike can also bind DC-SIGN (16), DC-
572 SIGNR (16), and L-SIGN (15). Similarly, TGEV binds to APN with the spike S1 CTD

Accepted Manuscript Posted Online

Journal of Virology

JVI

Journal of Virology

Downloaded from http://jvi.asm.org/ on August 6, 2016 by NORTHERN ILLINOIS UNIV

573 (10) but the virus is also capable of binding to cell surface sugars and sialic acids using
574 the N-terminal domain (NTD) of S1 (37). Since MHV binds CEACAM1 at the first 330
575 amino acids of the S1 NTD (38), one may postulate that MERS-CoV spike may similarly
576 bind CEACAM5 with the NTD of S1. In this regard, the CEACAM5-S1 NTD interaction
577 may orchestrate with the DPP4-S1 CTD interaction (36, 39) and facilitates the infection
578 of MERS-CoV. Importantly, the epitopes from the receptor-binding domain of MERS-
579 CoV S1 are known to trigger the production of potent neutralization antibodies. It is
580 potentially feasible to include additional epitopes derived from the CEACAM5-binding
581 domain in future vaccine designs, which may further enhance the efficiency of the
582 produced neutralizing antibodies at the same time avoiding potential immunopathological
583 effects as observed from using the full length spike protein (40).
584
585 By definition, a receptor is a cellular factor essential for viral entry and bound by the viral
586 glycoproteins whereas an attachment factor is a cellular factor that can increase the
587 efficiency of virus entry but is not sufficient to render otherwise refractory cells
588 susceptible to infection. In line with the definitions, CEACAM5 expression was
589 predominantly detected in cell types highly susceptible to MERS-CoV infection,
590 including Huh7, Calu3, and T cells. Therefore, the expression of CEACAM5 may in part
591 contribute to the permissiveness of a certain cell type in addition to DPP4. Our data
592 showed that the expression of CEACAM5 did not confer infectivity by MERS-CoV to
593 the non-permissive BHK21 cells. However, the expression of CEACAM5 markedly
594 increased the amount of virus particles that were bound to the cell surface. Subsequent
595 analyses confirmed that CEACAM5 expression could enhance MERS-CoV entry in

Accepted Manuscript Posted Online

Journal of Virology

JVI

Journal of Virology

Downloaded from http://jvi.asm.org/ on August 6, 2016 by NORTHERN ILLINOIS UNIV

596 AD293 cells, which expressed endogenous DPP4. Therefore, mechanistically CEACAM5
597 may help to concentrate the virus particles at the cell surface and render the virus
598 particles a higher accessibility to DPP4, which can then be used to initiate the cell entry
599 process.
600
601 In conclusion, in this study we identified CEACAM5 as a novel surface binding protein
602 for MERS-CoV that could facilitate MERS-CoV entry through serving as an important
603 attachment factor. This novel cell surface factor could be a potential antiviral target in the
604 combat against MERS-CoV infection.
605
606 **Acknowledgements.** We thank Professor Suet Yi Leung for providing the normal human
607 lung sections. We thank the staff at the Core Facility, Li Ka Shing Faculty of Medicine,
608 The University of Hong Kong, for facilitation of the study.
609
610 **Funding Information.** This work was partly supported by The Providence Foundation
611 Limited in memory of the late Dr. Lui Hac Minh, the Hong Kong Health and Medical
612 Research Fund (14131392 and 15140762), the NSFC/RGC Joint Research Scheme
613 (N_HKU728/14), the Theme-Based Research Scheme (T11/707/15) of the Research
614 Grants Council, Hong Kong Special Administrative Region, and funding from the
615 Ministry of Education of China for the Collaborative Innovation Center for Diagnosis and
616 Treatment of Infectious Diseases. The funding sources had no role in the study design,
617 data collection, analysis, interpretation, or writing of the report.
618

Accepted Manuscript Posted Online

Journal of Virology

JVI

Journal of Virology

Downloaded from http://jvi.asm.org/ on August 6, 2016 by NORTHERN ILLINOIS UNIV

619 **Potential conflicts of interest.** All authors: No reported conflicts.

620

621

622

623 **Reference**

624 1. **Chan JF, Lau SK, To KK, Cheng VC, Woo PC, Yuen KY.** 2015. Middle East
625 respiratory syndrome coronavirus: another zoonotic betacoronavirus
626 causing SARS-like disease. Clin Microbiol Rev **28:**465-522.
627 2. **Chan JF, To KK, Tse H, Jin DY, Yuen KY.** 2013. Interspecies transmission
628 and emergence of novel viruses: lessons from bats and birds. Trends
629 Microbiol **21:**544-555.
630 3. **Yeager CL, Ashmun RA, Williams RK, Cardellichio CB, Shapiro LH, Look**
631 **AT, Holmes KV.** 1992. Human aminopeptidase N is a receptor for human
632 coronavirus 229E. Nature **357:**420-422.
633 4. **Vlasak R, Luytjes W, Spaan W, Palese P.** 1988. Human and bovine
634 coronaviruses recognize sialic acid-containing receptors similar to those of
635 influenza C viruses. Proc Natl Acad Sci U S A **85:**4526-4529.
636 5. **Li W, Moore MJ, Vasilieva N, Sui J, Wong SK, Berne MA, Somasundaran M,**
637 **Sullivan JL, Luzuriaga K, Greenough TC, Choe H, Farzan M.** 2003.
638 Angiotensin-converting enzyme 2 is a functional receptor for the SARS
639 coronavirus. Nature **426:**450-454.
640 6. **Hofmann H, Pyrc K, van der Hoek L, Geier M, Berkhout B, Pohlmann S.**
641 2005. Human coronavirus NL63 employs the severe acute respiratory
642 syndrome coronavirus receptor for cellular entry. Proc Natl Acad Sci U S A
643 **102:**7988-7993.
644 7. **Huang X, Dong W, Milewska A, Golda A, Qi Y, Zhu QK, Marasco WA, Baric**
645 **RS, Sims AC, Pyrc K, Li W, Sui J.** 2015. Human Coronavirus HKU1 Spike
646 Protein Uses O-Acetylated Sialic Acid as an Attachment Receptor
647 Determinant and Employs Hemagglutinin-Esterase Protein as a Receptor-
648 Destroying Enzyme. J Virol **89:**7202-7213.
649 8. **Zaki AM, van Boheemen S, Bestebroer TM, Osterhaus AD, Fouchier RA.**
650 2012. Isolation of a novel coronavirus from a man with pneumonia in Saudi
651 Arabia. N Engl J Med **367:**1814-1820.
652 9. **Raj VS, Mou H, Smits SL, Dekkers DH, Muller MA, Dijkman R, Muth D,**
653 **Demmers JA, Zaki A, Fouchier RA, Thiel V, Drosten C, Rottier PJ,**
654 **Osterhaus AD, Bosch BJ, Haagmans BL.** 2013. Dipeptidyl peptidase 4 is a
655 functional receptor for the emerging human coronavirus-EMC. Nature
656 **495:**251-254.
657 10. **Delmas B, Gelfi J, L'Haridon R, Vogel LK, Sjostrom H, Noren O, Laude H.**
658 1992. Aminopeptidase N is a major receptor for the entero-pathogenic
659 coronavirus TGEV. Nature **357:**417-420.

Accepted Manuscript Posted Online

Journal of Virology

JVI

Journal of Virology

Downloaded from http://jvi.asm.org/ on August 6, 2016 by NORTHERN ILLINOIS UNIV

660 11. **Williams RK, Jiang GS, Holmes KV.** 1991. Receptor for mouse hepatitis
661 virus is a member of the carcinoembryonic antigen family of glycoproteins.
662 Proc Natl Acad Sci U S A **88:**5533-5536.
663 12. **Schultze B, Krempl C, Ballesteros ML, Shaw L, Schauer R, Enjuanes L,**
664 **Herrler G.** 1996. Transmissible gastroenteritis coronavirus, but not the
665 related porcine respiratory coronavirus, has a sialic acid (N-
666 glycolylneuraminic acid) binding activity. J Virol **70:**5634-5637.
667 13. **Schwegmann-Wessels C, Zimmer G, Schroder B, Breves G, Herrler G.**
668 2003. Binding of transmissible gastroenteritis coronavirus to brush border
669 membrane sialoglycoproteins. J Virol **77:**11846-11848.
670 14. **Milewska A, Zarebski M, Nowak P, Stozek K, Potempa J, Pyrc K.** 2014.
671 Human coronavirus NL63 utilizes heparan sulfate proteoglycans for
672 attachment to target cells. J Virol **88:**13221-13230.
673 15. **Jeffers SA, Tusell SM, Gillim-Ross L, Hemmila EM, Achenbach JE, Babcock**
674 **GJ, Thomas WD, Jr., Thackray LB, Young MD, Mason RJ, Ambrosino DM,**
675 **Wentworth DE, Demartini JC, Holmes KV.** 2004. CD209L (L-SIGN) is a
676 receptor for severe acute respiratory syndrome coronavirus. Proc Natl Acad
677 Sci U S A **101:**15748-15753.
678 16. **Marzi A, Gramberg T, Simmons G, Moller P, Rennekamp AJ, Krumbiegel**
679 **M, Geier M, Eisemann J, Turza N, Saunier B, Steinkasserer A, Becker S,**
680 **Bates P, Hofmann H, Pohlmann S.** 2004. DC-SIGN and DC-SIGNR interact
681 with the glycoprotein of Marburg virus and the S protein of severe acute
682 respiratory syndrome coronavirus. J Virol **78:**12090-12095.
683 17. **Chan CM, Lau SK, Woo PC, Tse H, Zheng BJ, Chen L, Huang JD, Yuen KY.**
684 2009. Identification of major histocompatibility complex class I C molecule as
685 an attachment factor that facilitates coronavirus HKU1 spike-mediated
686 infection. J Virol **83:**1026-1035.
687 18. **Zumla A, Chan JF, Azhar EI, Hui DS, Yuen KY.** 2016. Coronaviruses - drug
688 discovery and therapeutic options. Nat Rev Drug Discov **15:**327-347.
689 19. **Yeung ML, Yao Y, Jia, L, Chan, J.F., Chan K.H., Cheung, K.F., Chen, H.L.,**
690 **Poon, V.K., Tsang, A.K., To, K.K., Yiu, M.K., Teng, J.L., Chu, H., Zhou, J.,**
691 **Zhang, Q., Deng, W., Lau, S.K., Lau, J.Y., Woo, P.C., Chan, T.M., Yung, S.,**
692 **Zheng, B.J., Jin, D.Y., Mathieson, P.W., Qin, C., Yuen, K.Y.** 2016. MERS
693 coronavirus induces apoptosis in kidney and lung by upregulating Smad7
694 and FGF2. Nature Microbiology **1:**doi:10.1038/nmicrobiol.2016.1034.
695 20. **WHO.** http://www.who.int/csr/don/16-may-2016-mers-saudi-arabia/en/.
696 Accessed May.
697 21. **Assiri A, Al-Tawfiq JA, Al-Rabeeah AA, Al-Rabiah FA, Al-Hajjar S, Al-**
698 **Barrak A, Flemban H, Al-Nassir WN, Balkhy HH, Al-Hakeem RF,**
699 **Makhdoom HQ, Zumla AI, Memish ZA.** 2013. Epidemiological,
700 demographic, and clinical characteristics of 47 cases of Middle East
701 respiratory syndrome coronavirus disease from Saudi Arabia: a descriptive
702 study. Lancet Infect Dis **13:**752-761.
703 22. **Muller MA, Raj VS, Muth D, Meyer B, Kallies S, Smits SL, Wollny R,**
704 **Bestebroer TM, Specht S, Suliman T, Zimmermann K, Binger T, Eckerle I,**
705 **Tschapka M, Zaki AM, Osterhaus AD, Fouchier RA, Haagmans BL,**

Accepted Manuscript Posted Online

706 **Drosten C.** 2012. Human coronavirus EMC does not require the SARS-
707 coronavirus receptor and maintains broad replicative capability in
708 mammalian cell lines. MBio **3**.
709 23. **Chan JF, Chan KH, Choi GK, To KK, Tse H, Cai JP, Yeung ML, Cheng VC,**
710 **Chen H, Che XY, Lau SK, Woo PC, Yuen KY.** 2013. Differential cell line
711 susceptibility to the emerging novel human betacoronavirus 2c EMC/2012:
712 implications for disease pathogenesis and clinical manifestation. J Infect Dis
713 **207:**1743-1752.
714 24. **Zhou J, Chu H, Chan JF, Yuen KY.** 2015. Middle East respiratory syndrome
715 coronavirus infection: virus-host cell interactions and implications on
716 pathogenesis. Virol J **12:**218.
717 25. **Chu H, Zhou J, Wong BH, Li C, Chan JF, Cheng ZS, Yang D, Wang D, Lee AC,**
718 **Li C, Yeung ML, Cai JP, Chan IH, Ho WK, To KK, Zheng BJ, Yao Y, Qin C,**
719 **Yuen KY.** 2016. Middle East Respiratory Syndrome Coronavirus Efficiently
720 Infects Human Primary T Lymphocytes and Activates the Extrinsic and
721 Intrinsic Apoptosis Pathways. J Infect Dis **213:**904-914.
722 26. **Chan CM, Chu H, Zhang AJ, Leung LH, Sze KH, Kao RY, Chik KK, To KK,**
723 **Chan JF, Chen H, Jin DY, Liu L, Yuen KY.** 2016. Hemagglutinin of influenza A
724 virus binds specifically to cell surface nucleolin and plays a role in virus
725 internalization. Virology **494:**78-88.
726 27. **Zhou J, Chu H, Li C, Wong BH, Cheng ZS, Poon VK, Sun T, Lau CC, Wong**
727 **KK, Chan JY, Chan JF, To KK, Chan KH, Zheng BJ, Yuen KY.** 2014. Active
728 replication of Middle East respiratory syndrome coronavirus and aberrant
729 induction of inflammatory cytokines and chemokines in human
730 macrophages: implications for pathogenesis. J Infect Dis **209:**1331-1342.
731 28. **Chan JF, Yao Y, Yeung ML, Deng W, Bao L, Jia L, Li F, Xiao C, Gao H, Yu P,**
732 **Cai JP, Chu H, Zhou J, Chen H, Qin C, Yuen KY.** 2015. Treatment With
733 Lopinavir/Ritonavir or Interferon-beta1b Improves Outcome of MERS-CoV
734 Infection in a Nonhuman Primate Model of Common Marmoset. J Infect Dis
735 **212:**1904-1913.
736 29. **Chu H, Zhou J, Wong BH, Li C, Cheng ZS, Lin X, Poon VK, Sun T, Lau CC,**
737 **Chan JF, To KK, Chan KH, Lu L, Zheng BJ, Yuen KY.** 2014. Productive
738 replication of Middle East respiratory syndrome coronavirus in monocyte-
739 derived dendritic cells modulates innate immune response. Virology **454-**
740 **455:**197-205.
741 30. **van Doremalen N, Miazgowicz KL, Milne-Price S, Bushmaker T,**
742 **Robertson S, Scott D, Kinne J, McLellan JS, Zhu J, Munster VJ.** 2014. Host
743 species restriction of Middle East respiratory syndrome coronavirus through
744 its receptor, dipeptidyl peptidase 4. J Virol **88:**9220-9232.
745 31. **Hammarstrom S.** 1999. The carcinoembryonic antigen (CEA) family:
746 structures, suggested functions and expression in normal and malignant
747 tissues. Semin Cancer Biol **9:**67-81.
748 32. **Graham RL, Donaldson EF, Baric RS.** 2013. A decade after SARS: strategies
749 for controlling emerging coronaviruses. Nat Rev Microbiol **11:**836-848.

Journal of Virology

JVI

Journal of Virology

Downloaded from http://jvi.asm.org/ on August 6, 2016 by NORTHERN ILLINOIS UNIV

Accepted Manuscript Posted Online

33. **Han SU, Kwak TH, Her KH, Cho YH, Choi C, Lee HJ, Hong S, Park YS, Kim YS, Kim TA, Kim SJ.** 2008. CEACAM5 and CEACAM6 are major target genes for Smad3-mediated TGF-beta signaling. Oncogene **27:**675-683.
34. **Roda G, Jianyu X, Park MS, DeMarte L, Hovhannisyan Z, Couri R, Stanners CP, Yeretssian G, Mayer L.** 2014. Characterizing CEACAM5 interaction with CD8alpha and CD1d in intestinal homeostasis. Mucosal Immunol **7:**615-624.
35. **Tchoupa AK, Schuhmacher T, Hauck CR.** 2014. Signaling by epithelial members of the CEACAM family - mucosal docking sites for pathogenic bacteria. Cell Commun Signal **12:**27.
36. **Lu G, Wang Q, Gao GF.** 2015. Bat-to-human: spike features determining 'host jump' of coronaviruses SARS-CoV, MERS-CoV, and beyond. Trends Microbiol **23:**468-478.
37. **Li F.** 2015. Receptor recognition mechanisms of coronaviruses: a decade of structural studies. J Virol **89:**1954-1964.
38. **Kubo H, Yamada YK, Taguchi F.** 1994. Localization of neutralizing epitopes and the receptor-binding site within the amino-terminal 330 amino acids of the murine coronavirus spike protein. J Virol **68:**5403-5410.
39. **Du L, Zhao G, Kou Z, Ma C, Sun S, Poon VK, Lu L, Wang L, Debnath AK, Zheng BJ, Zhou Y, Jiang S.** 2013. Identification of a receptor-binding domain in the S protein of the novel human coronavirus Middle East respiratory syndrome coronavirus as an essential target for vaccine development. J Virol **87:**9939-9942.
40. **Du L, Tai W, Zhou Y, Jiang S.** 2016. Vaccines for the prevention against the threat of MERS-CoV. Expert Rev Vaccines doi:10.1586/14760584.2016.1167603**:**1-12.

Downloaded from http://jvi.asm.org/ on August 6, 2016 by NORTHERN ILLINOIS UNIV

Accepted Manuscript Posted Online

Journal of Virology

JVI

Journal of Virology

Downloaded from http://jvi.asm.org/ on August 6, 2016 by NORTHERN ILLINOIS UNIV

786

787

788

789

790 **Figure Legends**

791 **Figure 1. CEACAM5 is a cell surface binding protein of MERS-CoV.** (A) A549 and
792 NIH3T3 biotinylated cell membrane proteins were extracted, separated by 4-12%
793 gradient gel, and transferred to PVDF membrane. (B) Membrane proteins were probed
794 with MERS-S-pseudotyped virus followed by detection of virus binding by incubating
795 with immune serum directed against the MERS-CoV spike protein (lane 1). Non-
796 susceptible cell membrane extracts from NIH3T3 was included as a negative control
797 (lane 2). (C) The gel fractions corresponding to the positive signal at approximately
798 90kDa was cut, electro-eluted, and confirmed by VOPBA prior to submission for MS
799 protein identification. (D) The identified amino acid sequences and their corresponding
800 positions were illustrated. The position of CEACAM5 in (B) and (C) was indicated with
801 *.

802

803 **Figure 2. Surface expression of CEACAM5 on mammalian cells.** (A) The indicated
804 human cell lines were fixed in 4% paraformaldehyde and immunolabeled for surface
805 DPP4 and CEACAM5 expression. The shaded curve and the solid line represented
806 isotype and antigen-specific staining, respectively. The same fixation and
807 immunostaining procedures were performed for human primary T cells (B) as well as a
808 number of non-human mammalian cells (C). (D) The average percentage of

Accepted Manuscript Posted Online

Journal of Virology

JVI

Journal of Virology

Downloaded from http://jvi.asm.org/ on August 6, 2016 by NORTHERN ILLINOIS UNIV

809 DPP4/CEACAM5 positive cells was illustrated. (E) The average DPP4/CEACAM5 mean
810 fluorescent intensity (MFI) was quantified. Rabbit isotype IgG was used in place of
811 antigen-specific antibodies for the controls. Data in (D) and (E) represented mean and
812 standard deviation from three independent experiments.
813
814 **Figure 3. The expression of CEACAM5 in human lung tissues.** Immunostaining of
815 CEACAM5 and DPP4 were performed on paraffin slides of normal human lung tissues.
816 Representative images of CEACAM5 and DPP4 expression in various regions of the
817 human lung were illustrated, which included the bronchi (A), small airways (B), and
818 alveoli (C). Arrowheads indicated alveolar macrophages with CEACAM5 and DPP4 co-
819 expression. Bars represented 50μm.
820
821 **Figure 4. CEACAM 5 interacts with MERS-CoV spike.** (A) Surface and intracellular
822 expression of CEACAM5-V5 were verified with flow cytometry. (B) For co-IP, BHK21
823 cells were transfected with CEACAM5-V5 (lane 1 and lane 2) or empty vector (lane 3).
824 The cell lysate was immunoprecipitated with MERS-CoV-S1-FLAG (lane 1 and 3) or E.
825 coli bacterial alkaline phosphatase (BAP)-FLAG protein (lane 2) pre-adsorbed onto anti-
826 FLAG M2 agarose beads prior to SDS-PAGE. The protein complex was detected by
827 using the anti-FLAG antibody or the anti-V5 antibody. (C) Reciprocal co-IP was
828 performed using CEACAM5-V5 as the bait. Purified MERS-CoV-S1-FLAG (lane 1 and
829 3) or BAP-FLAG proteins (lane 2) were immunoprecipitated with overexpressed
830 CEACAM5-V5 or pcDNA-V5 protein pre-adsorbed onto anti-V5 sepharose beads.
831 Western blots were detected with the anti-FLAG or the anti-CEACAM5 antibody. (D)

Accepted Manuscript Posted Online

Journal of Virology

JVI

Journal of Virology

Downloaded from http://jvi.asm.org/ on August 6, 2016 by NORTHERN ILLINOIS UNIV

832 Endogenous co-IP was performed from MERS-CoV-infected or mock-infected Huh7 cell
833 lysates. Immunoprecipitation was performed using the rabbit anti-CEACAM5 antibody,
834 the rabbit anti-MERS-CoV spike antibody, or the rabbit isotype IgG. Western blots were
835 detected with the rabbit anti-MERS-CoV spike antibody or the rabbit anti-CEACAM5
836 antibody.
837
838 **Figure 5. CEACAM5-specific antibody blocks MERS-CoV entry and replication.**
839 (A) The antibody blocking assay was performed in Calu3 cells using MERS-S-
840 pseudotyped virus. Antibodies were diluted to 2 μg/ml and incubated with Calu3 cells for
841 1 hour at 37ºC. Pseudotyped viruses were then added at a ratio of 100 lentiviral particle
842 (LP) per cell for 1 hour. Luciferase activity was determined at 48 hours post infection and
843 was normalized to that of the mock-treated cells. (B) The antibody blocking assay was
844 performed in Calu3 cells using MERS-CoV. Calu3 cells were pre-incubated with
845 antibodies at the indicated concentrations for 1 hour at 37ºC. The cells were then
846 inoculated with MERS-CoV at 1 MOI for 1 hour at 37ºC in the presence of the
847 antibodies. After 1 hour, the cells were washed and harvested. MERS-CoV entry was
848 assessed with qPCR and the result was normalized to that of the mock-treated cells. (C)
849 Calu3 cells were treated with CEACAM5 antibody for a total of 2 hours during pre-
850 incubation and virus inoculation (-1 - 1) or after virus inoculation (1 - 3). MERS-CoV
851 entry was assessed with qPCR. (D) The antibody blocking assay was performed in Caco2
852 cells. (E and F) The impact of CEACAM5 inhibition on MERS-CoV replication was
853 investigated in Huh7 cells. Huh7 cells were pre-incubated with antibodies at 2 μg/ml for
854 1 hour at 37ºC. The cells were then inoculated with MERS-CoV at 0.0005 MOI for 1

Accepted Manuscript Posted Online

Journal of Virology

JVI

Journal of Virology

Downloaded from http://jvi.asm.org/ on August 6, 2016 by NORTHERN ILLINOIS UNIV

855 hour at 37ºC in the presence of the antibodies. At the end of the inoculation period, the
856 inoculum was replaced with culture media containing the indicated antibodies. Cell
857 lysates (E) and supernatants (F) were harvested at 1, 24, and 48 hours post infection. The
858 virus genome copy number was determined with qPCR. ND indicated that virus was not
859 detected in the corresponding samples. In all panels, data represented mean and standard
860 deviation from three independent experiments. Results from the anti-DPP4-, anti-
861 CEACAM5-, and control IgG-treated samples were compared with that of the mock-
862 treated samples. Statistical analyses were carried out using Student's *t*-test. Statistical
863 significance was indicated by asterisk marks when $p < 0.05$.
864
865 **Figure 6. CEACAM5 recombinant protein and siRNA knockdown of CEACAM5**
866 **inhibits MERS-CoV entry.** (A and B) MERS-CoV at 0.1 MOI was pre-incubated with
867 human recombinant proteins at the indicated concentrations for 1 hour at 37ºC. After the
868 pre-incubation, the protein-virus mix was added to Calu3 cells (A) or Huh7 cells (B) for 2
869 hours at 37ºC. The cell lysates were subsequently harvested for qPCR analysis. Human
870 recombinant DPP4 and human recombinant IgG were included as positive and negative
871 controls, respectively. Results from the human recombinant DPP4-, huamn recombinant
872 CEACAM5-, and control human recombinant IgG-treated samples were compared with
873 that of the mock-treated samples. (C) Huh7 cells were treated with CEACAM5 protein
874 for a total of 3 hours during pre-incubation and virus inoculation (-1 - 2) or after virus
875 inoculation (2 - 5). MERS-CoV entry was assessed with qPCR. (D) Huh7 cells were
876 treated with 100uM gene-specific or scrambled siRNA for two consecutive days. (E and
877 F) The reduction of surface CEACAM5 and DPP4 expression was summarized. (G)

Accepted Manuscript Posted Online

Journal of Virology

JVI

Journal of Virology

Downloaded from http://jvi.asm.org/ on August 6, 2016 by NORTHERN ILLINOIS UNIV

878 siRNA-treated Huh7 cells were then subjected to MERS-CoV infection at 1 MOI for 2
879 hours at 37ºC. Cell lysates were subsequently harvested for qPCR analysis and the result
880 was normalized to that of the mock-treated cells. Results from the DPP4 siRNA-,
881 CEACAM5 siRNA-, and scrambled siRNA-treated samples were compared with that of
882 the mock-treated samples. In all panels, data represented mean and standard deviation
883 from three independent experiments. Statistical analyses were carried out using Student's
884 *t*-test. Statistical significance was indicated by asterisk marks when $p < 0.05$.
885
886 **Figure 7. CEACAM5 is an attachment factor for MERS-CoV.** (A and B) To assess
887 whether CEACAM5 is important for MERS-CoV entry, human CEACAM5 was
888 overexpressed in BHK21 cells. Human CEACAM5-expressing BHK21 cells were then
889 challenged with MERS-CoV at 5 MOI for 2 hours at 37ºC. The inoculum was then
890 replaced with culture media and the cells were incubated for another 4 hours before
891 harvesting for flow cytometry. (C and D) To assess whether CEACAM5 is important for
892 MERS-CoV attachment, human CEACAM5-expressing BHK21 cells were challenged
893 with MERS-CoV at 30 MOI for 2 hours at 4ºC before harvesting for flow cytometry.
894 Human DPP4-expressing BHK21 cells were included as controls for both entry and
895 attachment assays. Data in (B) and (D) represented the percentage of MERS-CoV NP
896 positive BHK21 cells after infection with or without DPP4/CEACAM5-overepression. In
897 both panels, mean and standard deviation were derived from three independent
898 experiments. Statistical analyses were carried out using Student's *t*-test. Statistical
899 significance was indicated by asterisk marks when $p < 0.05$.
900

Accepted Manuscript Posted Online

Journal of Virology

JVI

Journal of Virology

Downloaded from http://jvi.asm.org/ on August 6, 2016 by NORTHERN ILLINOIS UNIV

901 **Figure 8. CEACAM5 overexpression does not confer infectivity by MERS-CoV to**
902 **non-permissive cells but enhances MERS-CoV entry in permissive cells.** (A and C)
903 To verify the role of CEACAM5 in MERS-CoV entry, human CEACAM5 was
904 overexpressed in BHK21 cells or AD293 cells. The cells were then challenged with
905 MERS-CoV at 1 MOI for 2 hours at 37ºC. After 2 hours, the cells were washed
906 extensively and harvested for qPCR analysis. (B and D) To verify the role of CEACAM5
907 in MERS-CoV attachment, human CEACAM5-expressing BHK21 cells or human
908 CEACAM5-expressing AD293 cells were challenged with MERS-CoV at 1 MOI for 2
909 hours at 4ºC. The cell lysates were then harvested for qPCR analysis. DPP4- and empty
910 vector (pcDNA3.1)-expressing BHK21 cells were included as controls. In all panels, data
911 represented mean and standard deviation from three independent experiments. Results
912 from the human DPP4-, human CEACAM5-, and empty vector-overexpressing samples
913 were compared with that of the mock-treated samples. Statistical analyses were carried
914 out using Student's *t*-test. Statistical significance was indicated by asterisk marks when p
915 < 0.05.
916
917 **Figure 9. CEACAM5 overexpression does not facilitate SARS-CoV entry in VeroE6**
918 **cells.** (A) VeroE6 cells were transfected with a CEACAM5-expressing plasmid or an
919 empty vector. (B) The cells were challenged with SARS-S-pseudovirus or VSV-G-
920 pseudovirus at a ratio of 100 lentiviral particle (LP) per cell for 1 hour. Luciferase
921 activity from CEACAM5-transfected VeroE6 cells was determined at 48 hours post
922 pseudovirus challenge and was normalized to that of the empty vector-transfected
923 VeroE6 cells. Mean and standard deviation in panel B were derived from three

Accepted Manuscript Posted Online

Journal of Virology

JVI

Journal of Virology

Downloaded from http://jvi.asm.org/ on August 6, 2016 by NORTHERN ILLINOIS UNIV

924 independent experiments. Statistical analyses were carried out using Student's *t*-test.

925 Statistical significance was indicated by asterisk marks when $p < 0.05$.

926

Accepted Manuscript Posted Online

Journal of Virology

JVI

Journal of Virology

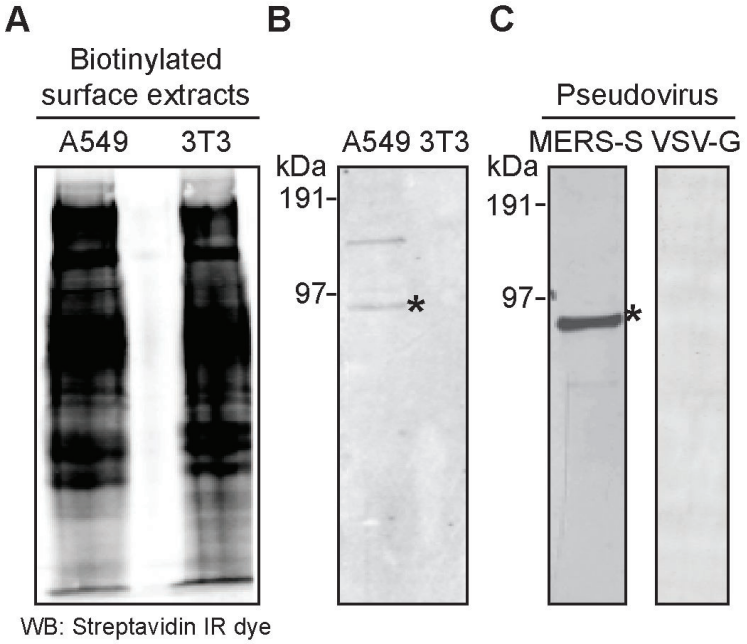

D

Tryptic peptide mass fingerprints

Amino Acid Sequence	Position
LTIESTPFNVAEGK	36-49
QIIGYVIGTQQATPGPAYSGR	78-98
SDLVNEEATGQFR	127-139
TLTLLSVTR	377-385
LSLSCHAASNP	433-443
TLTLFNVTR	555-563

Downloaded from http://jvi.asm.org/ on August 6, 2016 by NORTHERN ILLINOIS UNIV

Accepted Manuscript Posted Online

Journal of Virology

JVI

Journal of Virology

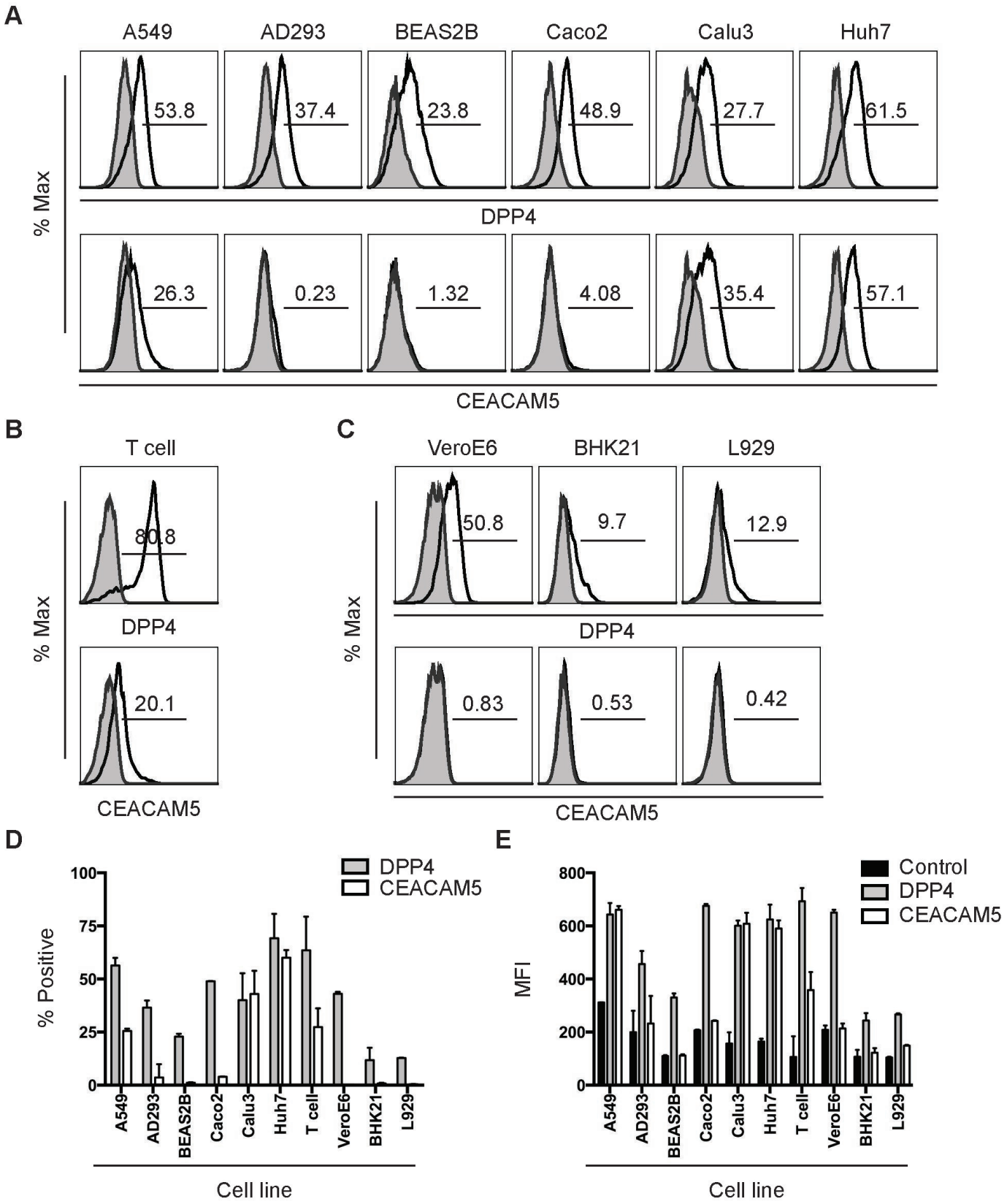

Downloaded from http://jvi.asm.org/ on August 6, 2016 by NORTHERN ILLINOIS UNIV

Accepted Manuscript Posted Online

Journal of Virology

JVI

Journal of Virology

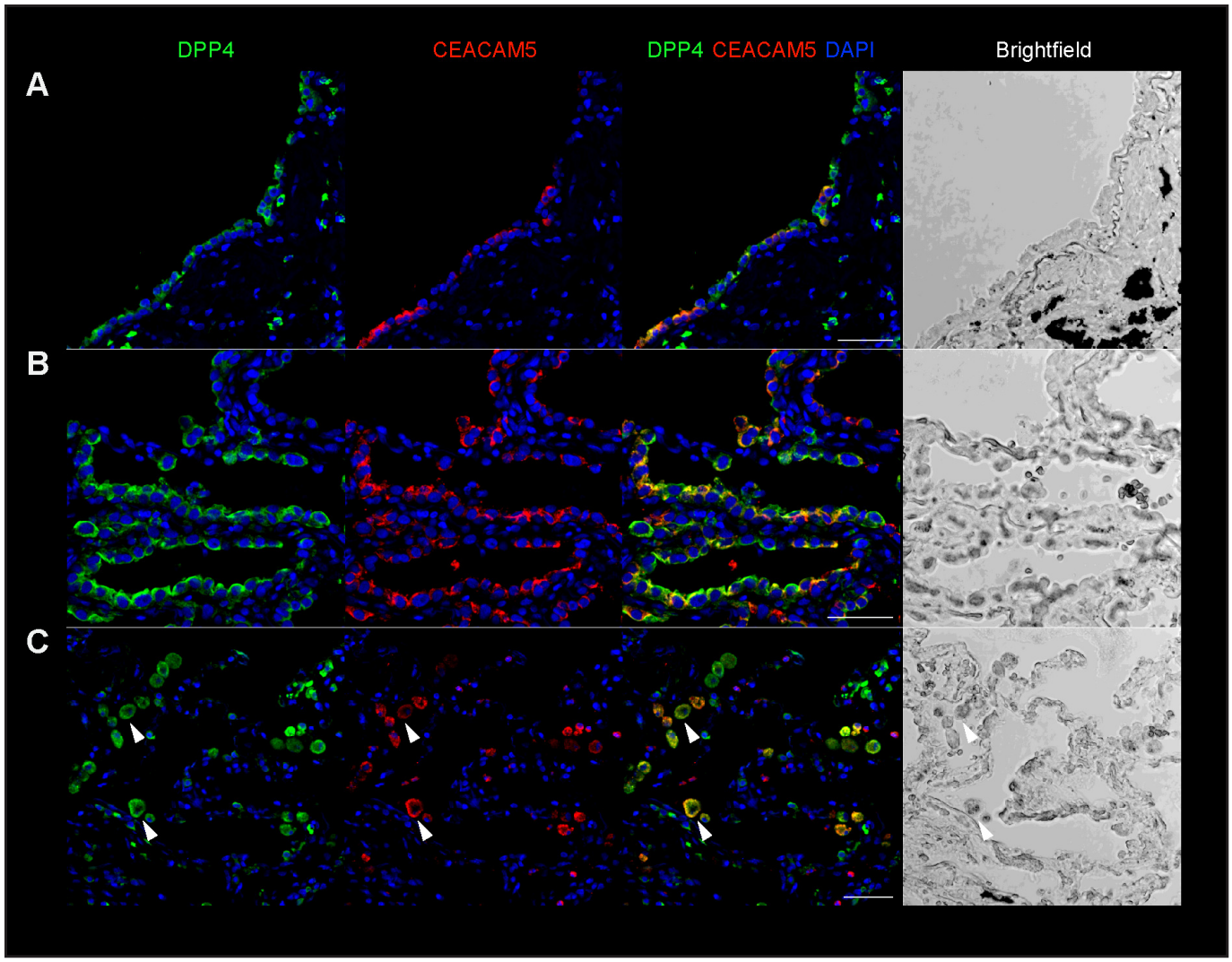

Downloaded from http://jvi.asm.org/ on August 6, 2016 by NORTHERN ILLINOIS UNIV

Accepted Manuscript Posted Online

Journal of Virology

JVI

Journal of Virology

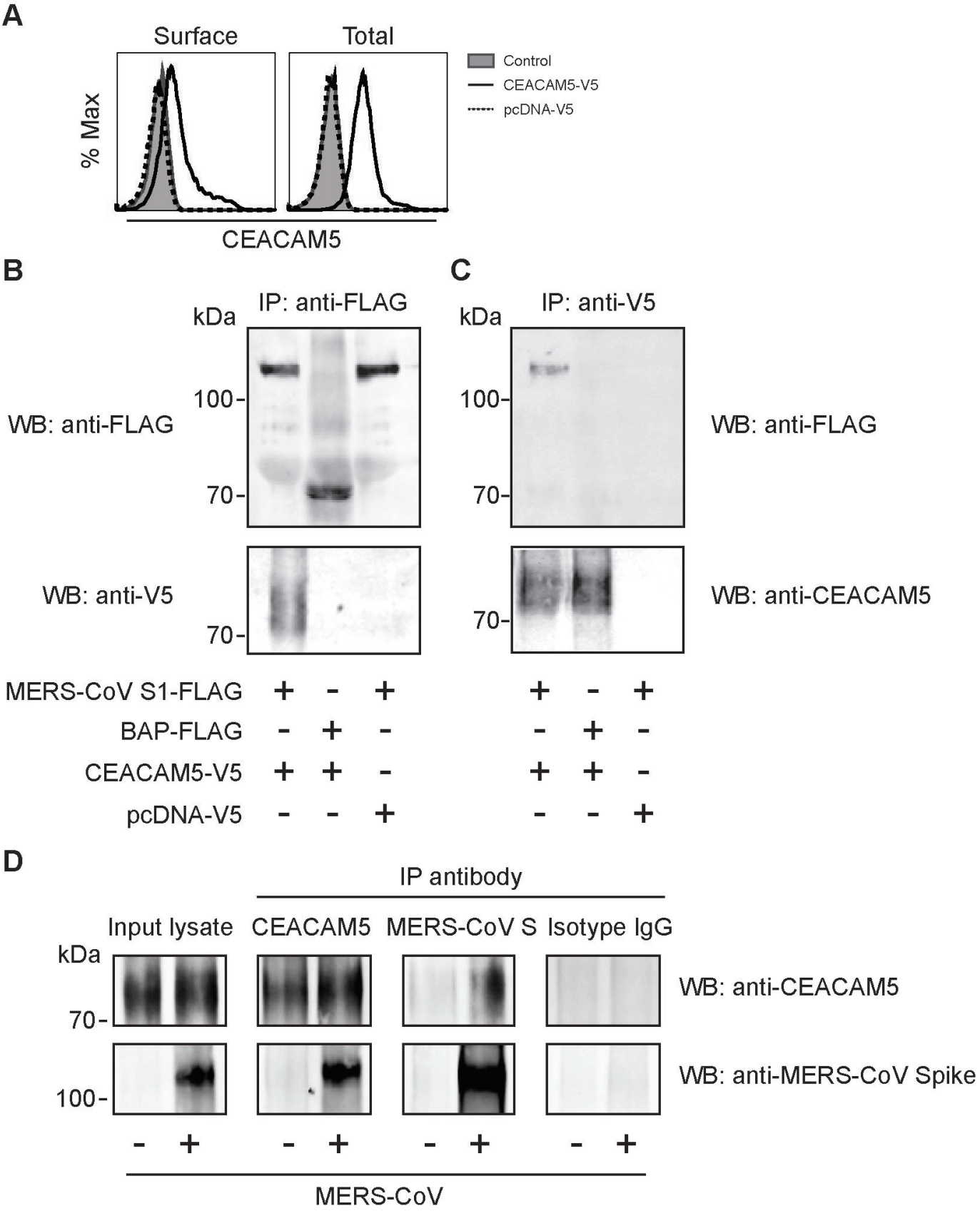

Downloaded from http://jvi.asm.org/ on August 6, 2016 by NORTHERN ILLINOIS UNIV

Accepted Manuscript Posted Online

Journal of Virology

JVI

Journal of Virology

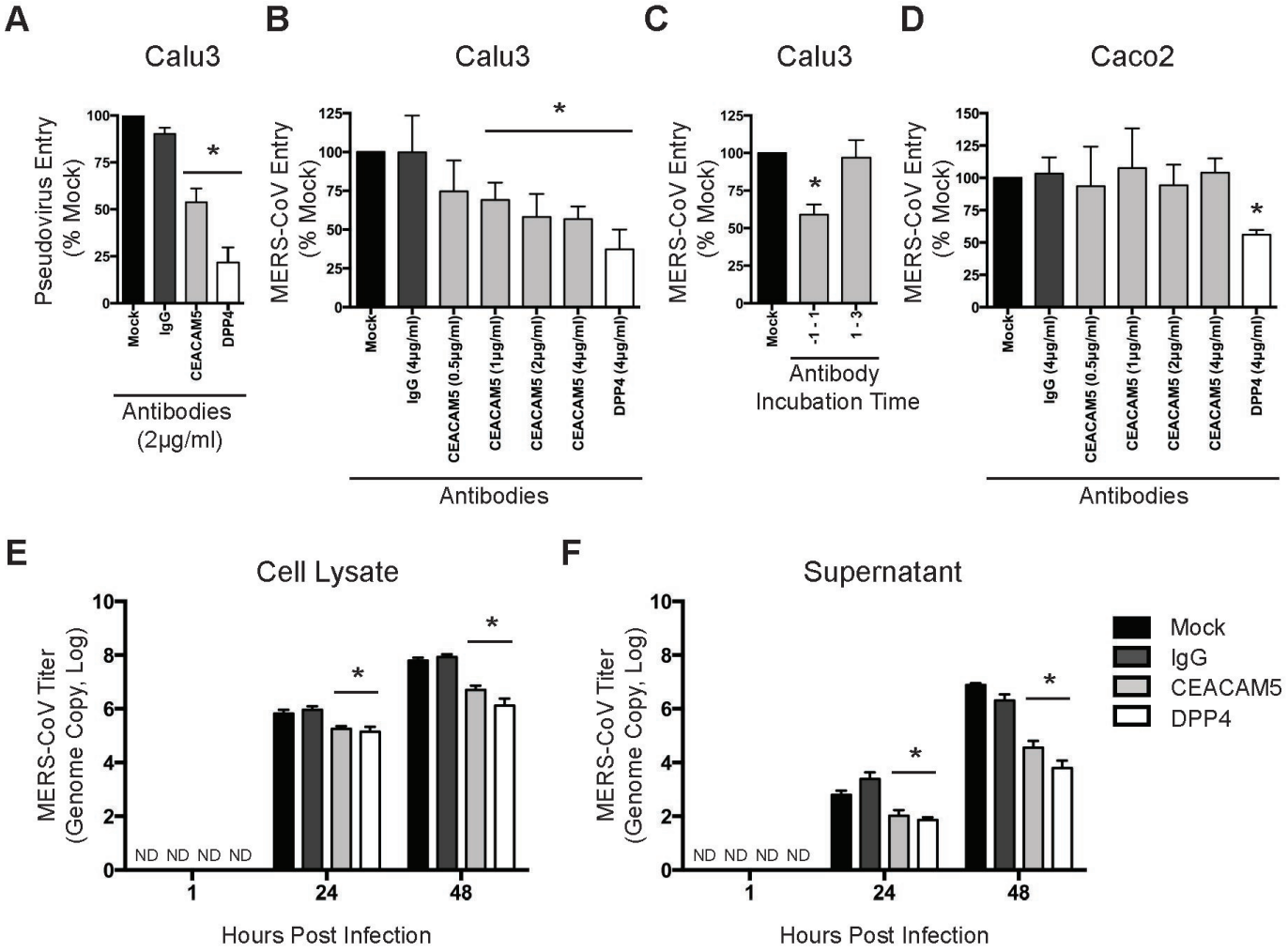

Downloaded from http://jvi.asm.org/ on August 6, 2016 by NORTHERN ILLINOIS UNIV

Accepted Manuscript Posted Online

Journal of Virology

JVI

Journal of Virology

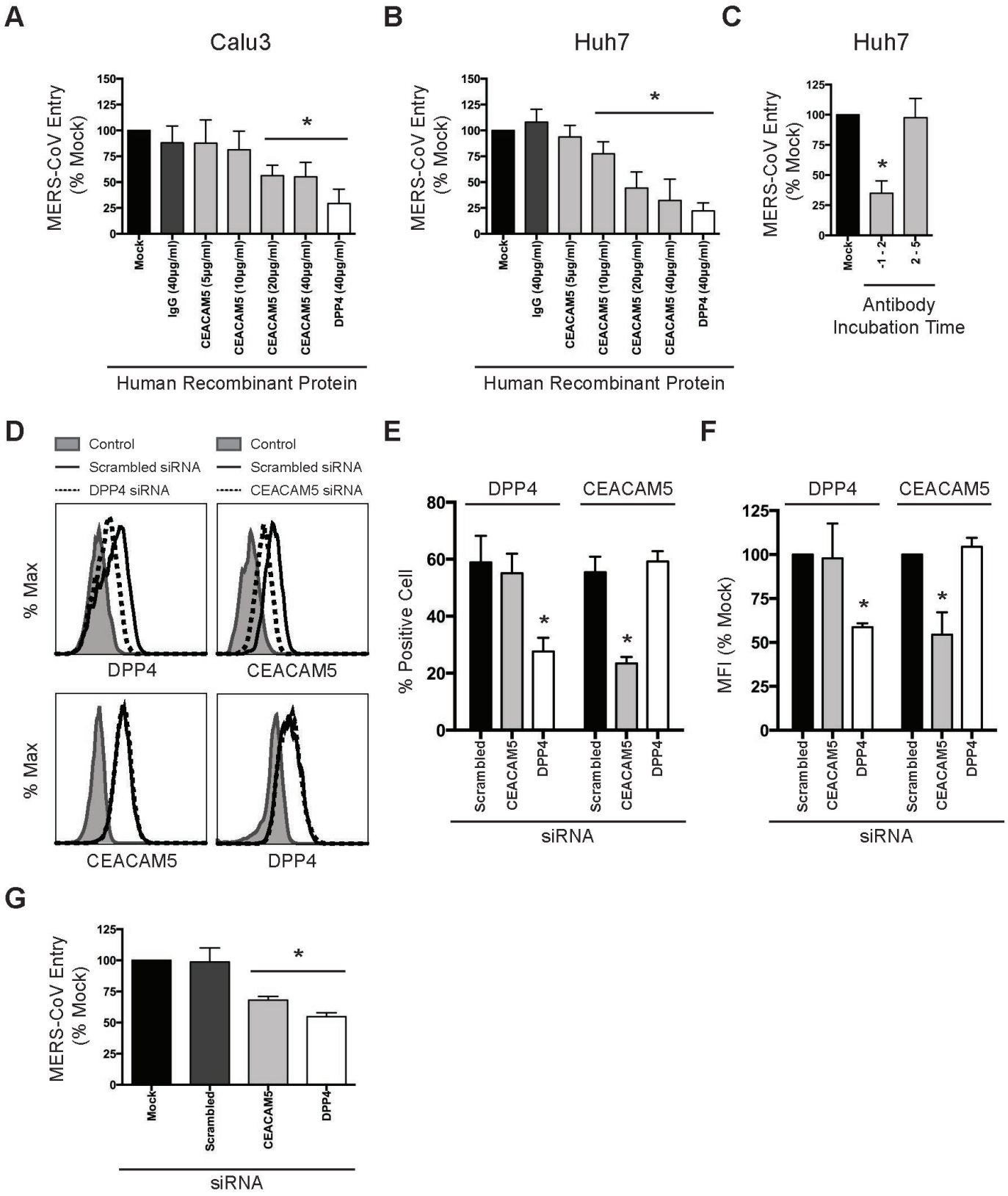

Downloaded from http://jvi.asm.org/ on August 6, 2016 by NORTHERN ILLINOIS UNIV

Accepted Manuscript Posted Online

Journal of Virology

JVI

Journal of Virology

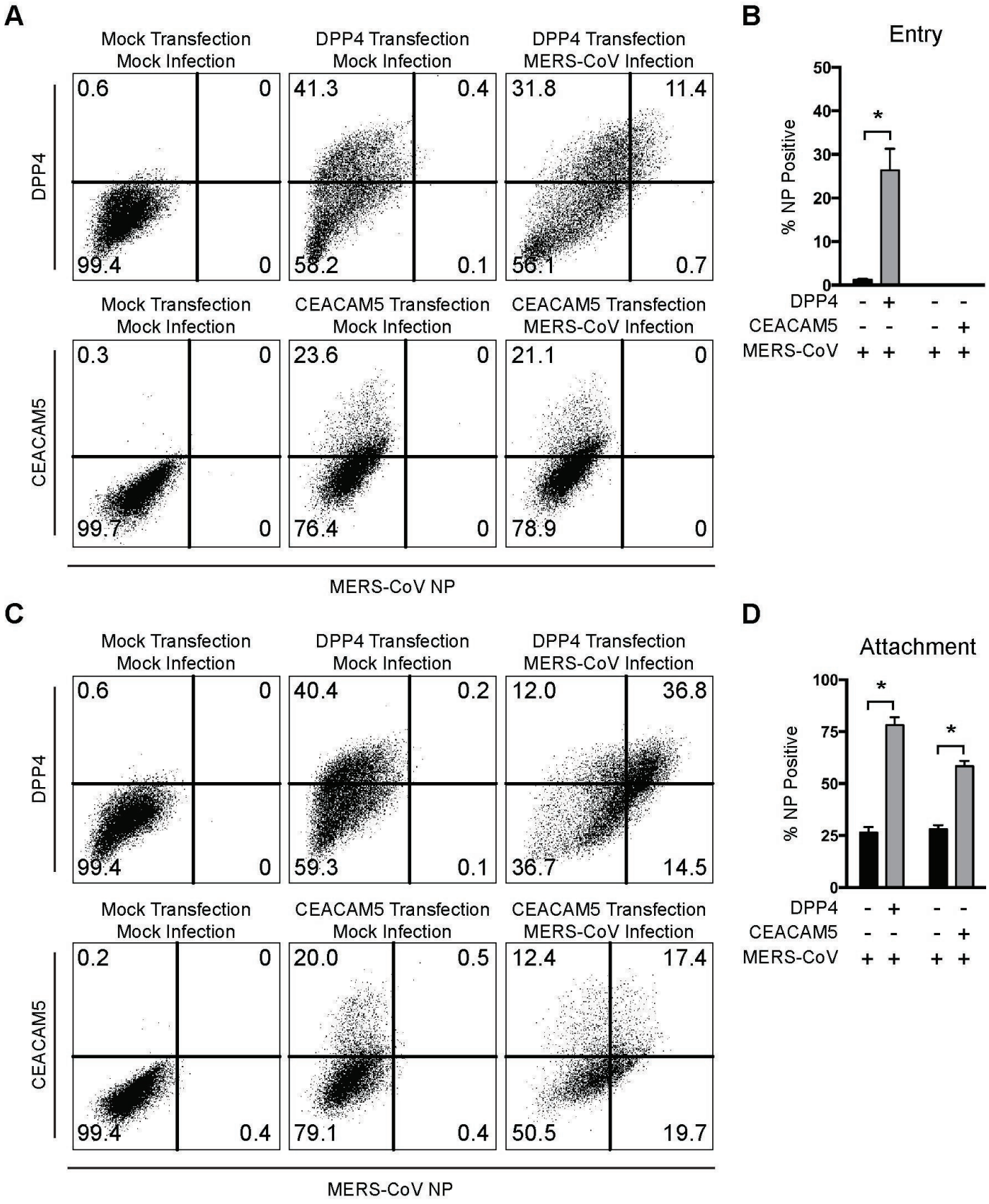

Downloaded from http://jvi.asm.org/ on August 6, 2016 by NORTHERN ILLINOIS UNIV

Accepted Manuscript Posted Online

Journal of Virology

JVI

Journal of Virology

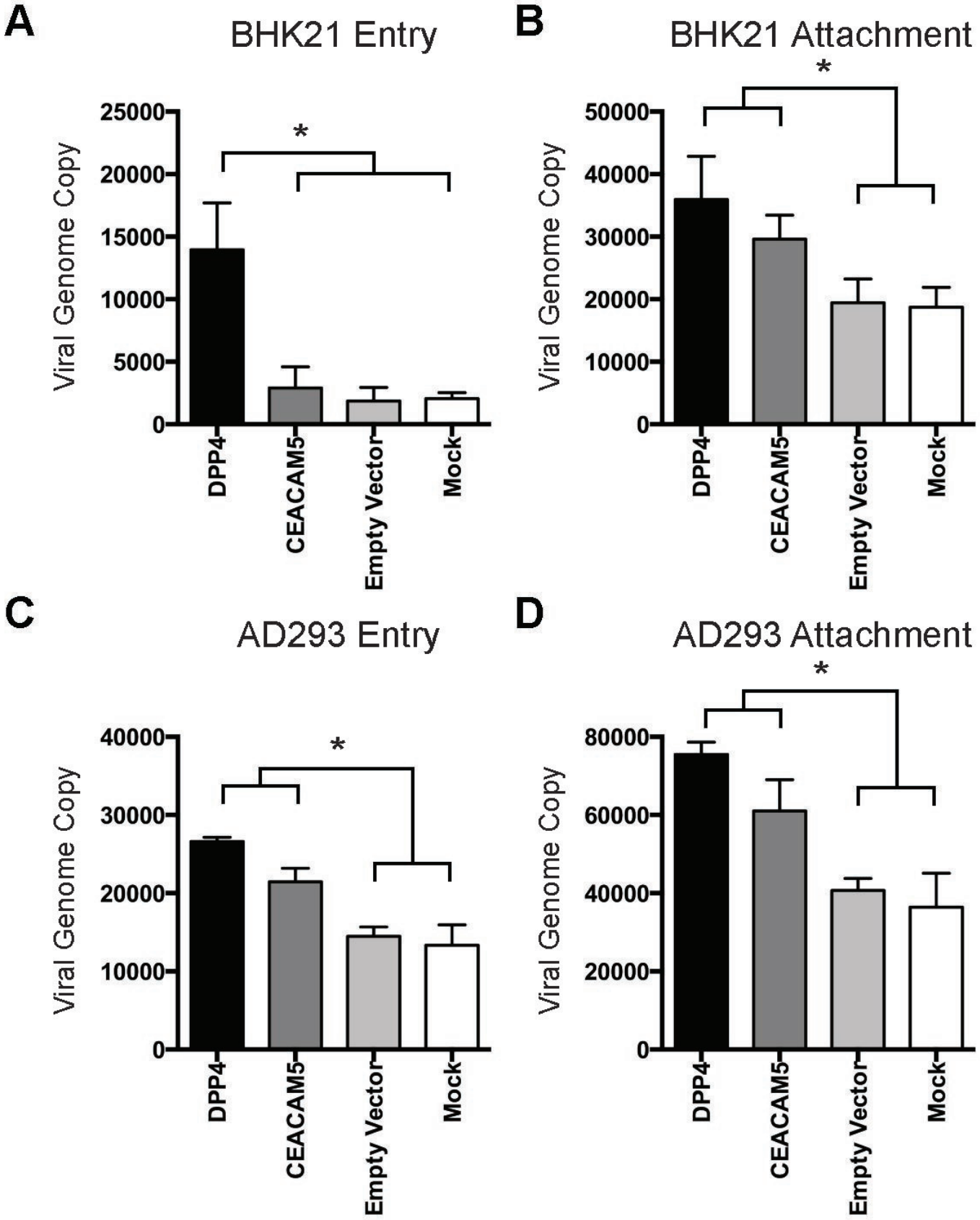

Downloaded from http://jvi.asm.org/ on August 6, 2016 by NORTHERN ILLINOIS UNIV

Accepted Manuscript Posted Online

Journal of Virology

JVI

Journal of Virology

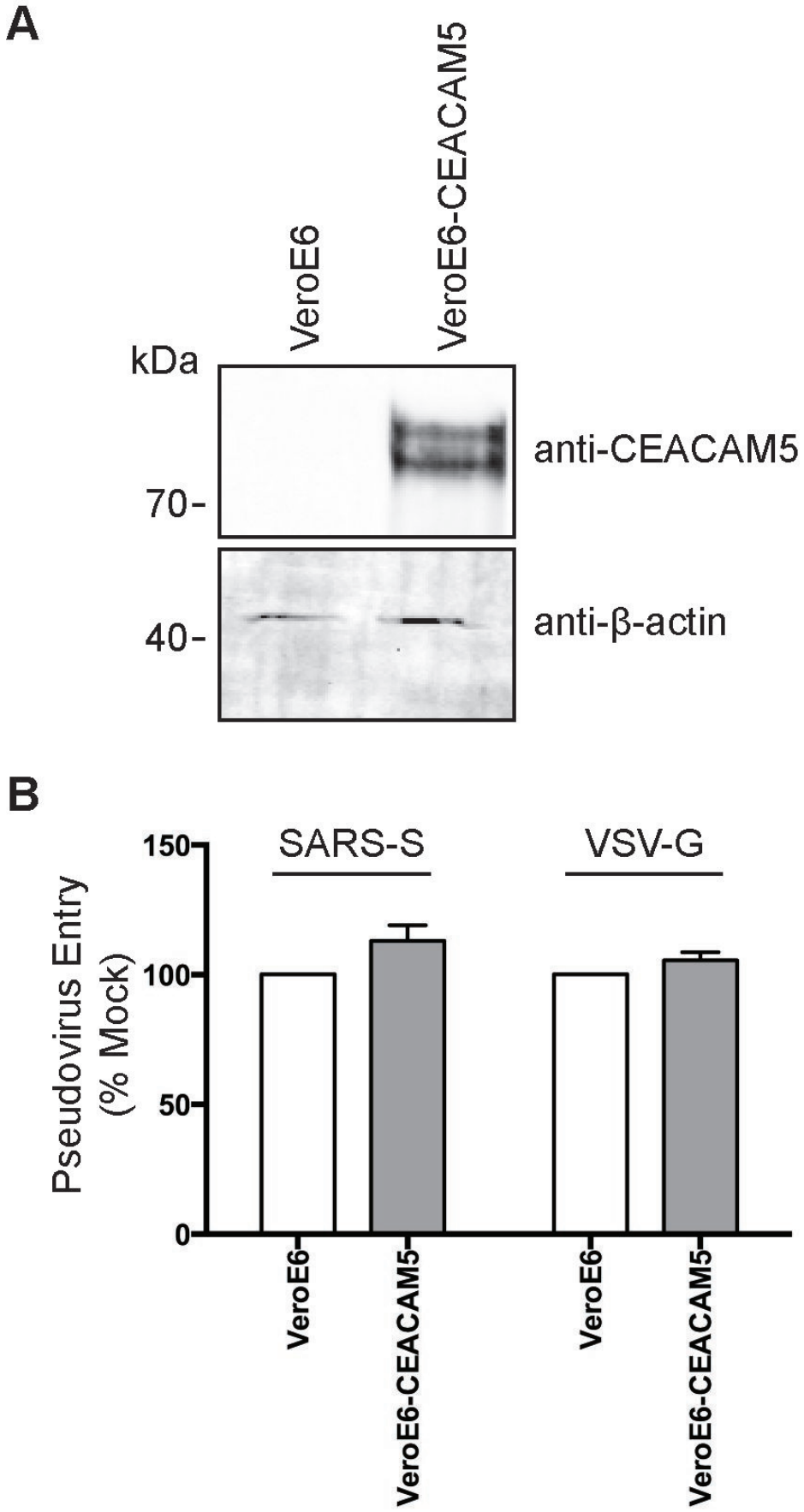

Downloaded from http://jvi.asm.org/ on August 6, 2016 by NORTHERN ILLINOIS UNIV